
Sequential Federated Learning in Hierarchical Architecture on Non-IID Datasets

Xingrun Yan

Beijing Institute of Technology
3220221473@bit.edu.cn

Shiyuan Zuo

Beijing Institute of Technology
zuoshiyuan@bit.edu.cn

Rongfei Fan

Beijing Institute of Technology
fanrongfei@bit.edu.cn

Han Hu

Beijing Institute of Technology
hhu@bit.edu.cn

Li Shen

Sun Yat-Sen University
shenli6@mail.sysu.edu.cn

Puning Zhao

Zhejiang Lab
pnzhao@zhejianglab.com

Yong Luo

Wuhan University
luoyong@whu.edu.cn

Abstract

In a real federated learning (FL) system, communication overhead for passing model parameters between the clients and the parameter server (PS) is often a bottleneck. Hierarchical federated learning (HFL) that poses multiple edge servers (ESs) between clients and the PS can partially alleviate communication pressure but still needs the aggregation of model parameters from multiple ESs at the PS. To further reduce communication overhead, we bring sequential FL (SFL) into HFL for the first time, which removes the central PS and enables the model training to be completed only through passing the global model between two adjacent ESs for each iteration, and propose a novel algorithm adaptive to such a combinational framework, referred to as Fed-CHS. Convergence results are derived for strongly convex and non-convex loss functions under various data heterogeneity setups, which show comparable convergence performance with the algorithms for HFL or SFL solely. Experimental results provide evidence of the superiority of our proposed Fed-CHS on both communication overhead saving and test accuracy over baseline methods.

1 Introduction

Recently, federated learning (FL) stands out as an emerging distributed ML approach that can alleviate the privacy concern of clients via multiple rounds of local training (Luo et al., 2022; Ma et al., 2022; Martínez Beltrán et al., 2023). In each round, participating clients first utilize their local data and the received FL global model in the last round to update their FL local models respectively, and then transmit the parameters of their most up-to-date local models to a parameter server (PS) (Wang et al., 2019; Li et al., 2022). Hereafter, the PS aggregates these uploaded local model parameters to have a new one and broadcasts it to each participating client. Convergence of global model can be promised in such a framework and no raw data is transmitted between any participating client and the PS (Gu et al., 2021; Collins et al., 2022; Song et al., 2023).

In traditional FL architecture, as the number of participating clients grows, it is very pricey to sustain a dedicated communication link between every client and the PS for global model updating, considering the data size of model parameter nowadays is generally enormous (WANG et al., 2019; Rothchild

et al., 2020; Luo et al., 2021; Shah and Lau, 2023; Amiri and Gündüz, 2020). To overcome this challenge, some efforts are made to reduce the number of bits to offload for each communication hop, e.g., through pruning the neural network model (Horváth et al., 2021; Zhang et al., 2022) or compressing the model parameter (Bibikar et al., 2022), etc. Differently, some other works try to save the number of communication hops by designing new aggregation mechanisms with a concern of network topology. *Hierarchical Federated Learning* (HFL) (Abad et al., 2020; Briggs et al., 2020; Lim et al., 2022) is such a kind of example that emerges recently. In HFL, massive clients are broadly distributed and have to get through the PS via an edge server (ES) in the vicinity. Dividing the set of clients into multiple clusters, within each of which there is an associated ES (Liu et al., 2020, 2023b; Wang et al., 2023). In any round of local model aggregation, each ES first aggregates the local models from the clients in its cluster and then pushes the aggregated one to the PS to generate the global model parameter (Yang, 2021; Ng et al., 2022; Qu et al., 2022; Liu et al., 2023a). Through this operation, the communication hops for offloading each client’s specific local model parameter from the associated ES node to the central PS are waived (Deng et al., 2021; Shi et al., 2021).

Even with HFL, the round-by-round aggregations of combined model parameters from every ES at the PS is still a communication-heavy task (Wang et al., 2021). This situation is even worse when the group of ESs and the PS are in a highly dynamic network, weakly interconnected, or subject to network topology mismatch, i.e., the topology of ESs and the PS is not in a stable and star shape (Pham et al., 2022; Zhou et al., 2023). To overcome this challenge, the idea of *sequential FL* (SFL) that removes PS from the FL system and allows global model parameters updated among participating clients sequentially, can serve as an enhancement, but has not been brought into HFL in literature. To leverage SFL in the framework of HFL, aggregated model parameter is updated sequentially among ESs, which exempts the parallel offloading of each ES to the PS (Sun et al., 2022; Ayache et al., 2023). The combination of HFL and SFL is adaptive to a broad range of network topologies. Some exemplary applications include, but are not limited to, Internet of Vehicles (IoV) and Integrated Low-earth Orbit (LEO) Satellite-Terrestrial Network, whose detailed descriptions are listed in Appendix D.

In addition, datasets from disjoint participating clients may be non-independent and identically distributed (non-IID) (or say be subject to data heterogeneity) due to diverse geographical environments and client characteristics (Liu et al., 2023b; Collins et al., 2022). Non-IID datasets bring new challenges into convergence proving for training algorithms and have been a vital issue to address in the traditional framework of FL, HFL, or SFL (Sun et al., 2022; Liu et al., 2023b; Song et al., 2023). In our combinational framework of SFL and HFL, the factor of non-IID cannot be ignored either as the HFL structure enables the coverage of a broader range of clients. How to promise convergence in such a situation is still an open problem, and cannot be answered based on existing related works that cares SFL or HFL sorely (Parsons et al., 2023; Liu et al., 2023a).

In this paper, to save communication hops and overcome the data heterogeneity that are widely existed, we investigate the realization of federated learning in the combinational framework of HFL and SFL with non-IID data sets, and propose a novel aggregation algorithm named Fed-CHS. In Fed-CHS, iterative training is performed cluster-by-cluster. For the currently active cluster, each client in it only needs to interact with the associated ES node, who then generates the most up-to-date global model parameter from these interactions and pushes the generated model parameter to the ES node in a neighbor cluster for next round of iteration. The selection of next passing ES node is realized based on a deterministic and simple rule. Rigorous convergence analysis is expanded when the loss function is strongly convex and non-convex, under various setup of data heterogeneity.

Contributions: Our main contributions are three-fold:

- **Algorithmically**, we investigate the combinational framework of SFL and HFL for the first time and propose a new aggregation algorithm Fed-CHS to be adaptive to it. Fed-CHS offers a communication overhead saving method compared with existing methods for HFL architecture or conventional FL framework and is totally different from existing communication-efficient methods that merely save the number of bits for each communication hop. Furthermore Fed-CHS is general to network topology, especially when the topology is highly dynamic or not in a star shape.
- **Theoretically**, we explore the convergence performance of Fed-CHS when the loss function is strongly convex or non-convex. Specifically, Fed-CHS can converge at a linear rate with T and a rate $O(1/K^{q-1})$ for $q \geq 2$ with K , which defines the rounds of training iteration among clusters and within a cluster respectively, for strongly convex loss function, and a rate of $O(1/T^{1+q_1-q_2})$

with $1 + q_1 > q_2$ and $q_2 \geq q_1$ for non-convex loss function under general data heterogeneity. Additionally, when data heterogeneity fades away partly or completely, Fed-CHS can further achieve zero optimality gap for strongly convex loss function, and stationary point for non-convex loss function, respectively, while keeping the convergence rate unchanged. These convergence results are comparable with the algorithms for HFL or SFL solely.

- **Numerically**, we conduct extensive experiments to compare Fed-CHS with baseline methods. The results verify the advantage of our proposed Fed-CHS in test accuracy and communication overhead saving.

2 Related Work in Brief

FL was firstly introduced in McMahan et al. (2017) and then evolves to be HFL or SFL for the sake of relieving communication overhead. Optimality gap and convergence rate are the two most analytical performance metrics in literature under diverse assumptions on loss function’s convexity, especially for non-IID dataset, which are surveyed briefly in the following. More details about the surveyed literature are given in Appendix E.

Hierarchical Federated Learning (HFL) In the framework of HFL, Tu et al. (2020) concerns limited computation capability at clients, Hosseinalipour et al. (2022) cares a special network connection topology like device-to-device (D2D), and Wang et al. (2023) takes communication bottleneck into account by allowing ES currently having bad link condition with the PS to delay the uploading of model parameter. However, Wang et al. (2023) still requires each ES to offload aggregated model parameter to the PS. Heavy parameter offloading task is only postponed rather than diminished in Wang et al. (2023).

Sequential Federated Learning (SFL) With regard to SFL, the *Next Passing Node* that is going to receive the most up-to-date global model parameter, may be selected by following a fixed order or randomly. When the next passing node is chosen by following a fixed order, ring topology has to be imposed (Wang et al., 2022; Zaccone et al., 2022), which can hardly accommodate to various network topology in real application. When the next passing node is selected in a random way, more computation overhead may be brought in for evaluating the Lipschitz constant as required in Ayache and El Rouayheb (2019) or the value function for working about an multiple armed bandit (MAB) problem in Ayache et al. (2023).

Convergence Guarantees for Federated Learning In terms of convergence analysis concerning data heterogeneity, for HFL, convex loss function is mainly concerned (Tu et al., 2020; Hosseinalipour et al., 2022; Wang et al., 2023). Some literature, including Tu et al. (2020); Wang et al. (2023), cannot achieve zero optimality gap but is able to converge at linear rate, for a general convex (Tu et al., 2020; Wang et al., 2023) or strongly convex (Wang et al., 2023) loss function. Hosseinalipour et al. (2022) can achieve zero optimality gap but at a convergence rate of $\mathcal{O}(1/T)$. However, the zero optimality gap in Hosseinalipour et al. (2022) is build on some special assumption on quantitative relationship between instant gradient of loss function and system parameter. While, for SFL, the aforementioned Mao et al. (2020); Ayache et al. (2023) have tried to overcome data heterogeneity. The loss function is assumed to be strongly convex in Mao et al. (2020); Ayache et al. (2023). Mao et al. (2020) can achieve convergence at rate $\mathcal{O}(1/T^{1-q})$ for $q \in (0, 1/2)$, while Ayache et al. (2023) is able to further achieve zero optimality gap at at rate $\mathcal{O}(1/\sqrt{T})$, which relies on the holding of a special condition between local model parameter and local gradient in the stage of initialization.

In summary, as the architecture evolves from conventional FL, the results of which is given in Appendix E, to HFL and SFL, i.e., from simple to complex, it becomes harder and harder to get ideal results for a general convex or non-convex loss function in front of heterogeneous dataset. In this situation, deriving analytical results under the combinational framework of HFL and SFL is even more challenging.

3 Fed-CHS

In this section, we present Fed-CHS. We first elaborate the problem setup under the hybrid framework of SFL and HFL.

3.1 Problem Setup

FL learning task: Consider a FL system with N clients. These N participating clients compose the set of $\mathcal{N} \triangleq \{1, 2, \dots, N\}$. For any participating client, say n th client, it has a local data set \mathcal{D}_n with D_n elements. The i th element of \mathcal{D}_n is a ground-true label $z_{n,i} = \{x_{n,i}, y_{n,i}\}$. The $x_{n,i} \in \mathcal{R}^{\text{in}}$ is the input vector and $y_{n,i} \in \mathcal{R}^{\text{out}}$ is the output vector. By utilizing the data set \mathcal{D}_n for $n \in \mathcal{N}$, we aim to train a d -dimension vector w by minimizing the following loss function

$$F(w) \triangleq \frac{1}{D_A} \sum_{n \in \mathcal{N}} \sum_{z_{n,i} \in \mathcal{D}_n} f(w, z_{n,i}) = \sum_{n \in \mathcal{N}} \frac{D_n}{D_A} f_n(w) \quad (1)$$

where $f(w, z_{n,i})$ is the loss function to evaluate the error for approximating $y_{n,i}$ with an input of $x_{n,i}$ and a selection of w , D_A is defined as $D_A \triangleq \sum_{n \in \mathcal{N}} D_n$, and $f_n(w)$ represents the local loss function of n th client, defined as

$$f_n(w) \triangleq \frac{1}{D_n} \sum_{z_{n,i} \in \mathcal{D}_n} f(w, z_{n,i}), \forall n \in \mathcal{N}. \quad (2)$$

For the ease of presentation in the following, with a randomly set $\xi_n \subseteq \mathcal{D}_n$, we define

$$f(w, \xi_n) \triangleq \frac{1}{|\xi_n|} \sum_{z_{n,i} \in \xi_n} f(w, z_{n,i}), \forall n \in \mathcal{N}. \quad (3)$$

Denoting γ_n as $\gamma_n = D_n/D_A$ for $n \in \mathcal{N}$, the training task can be reformulated as the following optimization problem

$$\min_{w \in \mathcal{R}^d} \left\{ F(w) \triangleq \sum_{n=1}^N \gamma_n f_n(w) \right\} \quad (4)$$

Accordingly, the gradient of loss function of $f_n(w)$, $f(w, \xi_n)$ with respect to w can be written as $\nabla f_n(w)$ or $\nabla f(w, \xi_n)$, and the gradient of global loss function $F(w)$ with respect to w is denoted as $\nabla F(w)$.

In a traditional framework of FL, to find the solution of the problem in Equation (4), a PS is obligated to interact with the involved clients iteratively round by round by exchanging the loss function's gradient or model parameter. This will lead to extremely heavy burden considering the model parameter is usually with high dimension. A FL training framework that can save the exchanging of loss function's gradient or model parameter is highly desirable.

Hybrid framework of SFL and HFL:

In this work, we adopt a communication-efficient hierarchical architecture. As shown in Fig. 1, the group of N clients are divided into M clusters, which compose the set $\mathcal{M} \triangleq \{1, 2, \dots, M\}$. For m th cluster, the set of associated clients are denoted as \mathcal{N}_m , and there is one ES that can interact with the clients in set \mathcal{N}_m , which is denoted as m th ES node. The group of M ES nodes are connected through communication links. In previous HFL works, to approximate the training process of traditional FL and to fulfill the advantage of communication-efficiency for this hierarchical architecture, in t th round, the local gradients $\nabla f_n(w^t)$ or $\nabla f(w^t, \xi_n)$ for $n \in \mathcal{N}_m$ can be firstly aggregated at m th ES to obtain an aggregated model parameter w_m^t for every $m \in \mathcal{M}$, and then form to be a global w^{t+1} through aggregating the set of $\{w_m^t | m \in \mathcal{M}\}$ at a PS. Once a global w^{t+1} is generated, it will be broadcasted

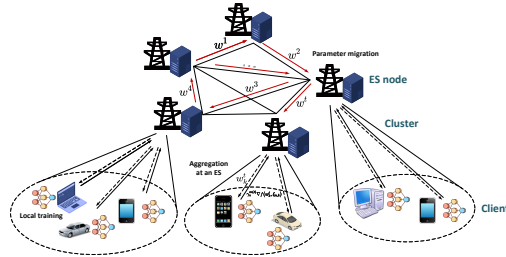


Figure 1: The framework of SFL in hierarchical architecture. In this architecture, clients are divided into multiple clusters, each of which is managed by one ES. For each step of iteration, model parameter is firstly updated within one cluster through multiple interactions between the ES and the associated clients, and then migrated to a neighbor ES (cluster) for next step of iteration.

to every client in each cluster through the associated ES. In such a procedure, the communication burden of uploading every specific $\nabla f_n(w^t)$ or $\nabla f(w^t, \xi_n)$ for $n \in \mathcal{N}_m$ via m th ES to the PS is saved. Bursty connecting requests from each client to the PS is also evaded.

To achieve better communication-efficiency, by referring to the framework of SFL, we do not assume the existence of PS and waive all the ES's from aggregating $\{w_m^t | m \in \mathcal{M}\}$ to be a global one like w^{t+1} in any round t . To be specific, for round t , only one selected ES, say $m(t)$ th ES, first broadcasts its received most up-to-date model parameter by round $(t-1)$, denoted as w^t for the ease of presentation, to all the clients in its cluster, i.e., $m(t)$ th cluster, and then aggregates the local gradients in its cluster, i.e., $\nabla f_n(w^t)$ or $\nabla f(w^t, \xi_n)$ for $n \in \mathcal{N}_m$ by some rule, to obtain an aggregated model parameter w^{t+1} . At the ending stage of round t , m th ES selects a new ES to work as the model parameter broadcaster and aggregator in round $(t+1)$, say $m(t+1)$ th ES, and push the most up-to-date model parameter w^{t+1} to $m(t+1)$ th ES.

Design goal: Under the above combinational framework of SFL and HFL, our goal is to design a proper aggregating rule at ES side and select a suitable $m(t+1)$ for each round t , so as to achieve convergent or optimal solution of the problem in Equation (4) as quickly as possible, while being robust to data heterogeneity.

3.2 Algorithm Description

To achieve our design goal, we develop Fed-CHS. In each training round of Fed-CHS, there is only one cluster being active, within which clients and the ES interacts multiple times to leverage the local dataset at these clients to update the global model parameter. With the global model parameter updated, the ES in currently active cluster selects the next passing cluster (and ES) by some rule and then push the most up-to-date global model parameter to it, in preparation for next round of training. Below, we give a full description of Fed-CHS (see Algorithm 1). Its crucial steps are explained in detail as follows.

- **Training within in one cluster:** In t th round, after receiving the global model parameter w^t that is broadcasted from $m(t)$ th ES, K times of interactions between $m(t)$ th ES and all the clients in set \mathcal{N}_m is activated. In k th step, suppose the global model parameter already known by each client at the beginning of this step is w_k^t , client n with $n \in \mathcal{N}_{m(t)}$ will updates its local model parameter based on a randomly selected dataset $\xi_{n,k} \subseteq \mathcal{D}_n$, and then return its gradient $\nabla f(w_k^t, \xi_{n,k})$ to ES $m(t)$. For ES $m(t)$, it first aggregates these received local gradients with weighting coefficients $\gamma_n^{m(t)}$ such that $\sum_{n \in \mathcal{N}_{m(t)}} \gamma_n^{m(t)} = 1$, then use the learning rate η_k to generate w_{k+1}^t , and finally broadcasts w_{k+1}^t to every client in its cluster. Specifically, w_{k+1}^t can be written as

$$w_{k+1}^t = w_k^t - \eta_k \sum_{n \in \mathcal{N}_{m(t)}} \gamma_n^{m(t)} \nabla f(w_k^t, \xi_{n,k}), k \in \mathcal{K} \triangleq \{0, 1, \dots, K-1\}. \quad (5)$$

With the iterative expression of w_k^t in Equation (5), there is $w_0^{t+1} = w^{t+1} = w_K^t$.

- **The selection of next passing cluster:** To select the next passing cluster, i.e., $m(t+1)$ th cluster, in case Fed-CHS has run t rounds of iterations, we propose to select $m(t+1)$ from $\mathcal{A}(m(t))$ by the following two-step rule. **Step 1:** Generate the set $\mathcal{C}(t) = \{m' | m' = \arg \min c(m'), m' \in \mathcal{A}(m(t))\}$. The set $\mathcal{C}(t)$ actually represents the set of ES nodes that is least traversed in last t rounds of iteration. If $|\mathcal{C}(t)| = 1$, suppose $\mathcal{C}(t) = m^\dagger$, output $m(t) = m^\dagger$. If $|\mathcal{C}(t)| > 1$, go to Step 2; **Step 2:** Set $m^\ddagger = \arg \max_{m' \in \mathcal{C}(t)} D_{A,m'}$, output $m(t+1) = m^\ddagger$. This operation is to select

the cluster with the largest dataset from $\mathcal{C}(t)$. The essence of above two-step rule is to drive the learning process to cover a broader range of dataset or more diversely distributed dataset.

Communication Overhead: With regard to communication burden for passing model parameters or gradients between ES nodes and clients, suppose we need Q bits to quantize a model parameter vector or local gradient vector, both of which is a d dimensional vector of floating numbers. For T round of iterations, suppose the maximal $|\mathcal{N}_m|$ for $m \in \mathcal{M}$ is N_{\max} , according to Algorithm 1, the clients need to upload $TKQN_{\max}$ bits at most to ES nodes, reversely the ES nodes broadcast TK times to deliver no exceeding $TKQN_{\max}$ bits to their associated clients, and TQ bits is required to transmitted among neighbor ES nodes.

Algorithm 1: Fed-CHS Algorithm

```

1: Input: Initial global model parameter  $w^0$ , client set  $\mathcal{N}$ , ES node set  $\mathcal{M}$ , the number of global iteration rounds  $T$ , the number of local iteration rounds  $K$ .
2: Output: Updated global model parameter  $w^T$ .
3: %% Initialization
4: ES  $m$  builds set  $\mathcal{N}_m$ , calculates  $D_{A,m}$ , and establish set  $\mathcal{A}_m$ , for  $m \in \mathcal{M}$ . Set  $M$ -dimensional vector  $c = (0, \dots, 0)^T$ . Randomly select  $m(0)$  from set  $\mathcal{M}$  and set  $w_0^0 = w^0$ .
5: for  $t = 0: T - 1$  do
6:   %% Training within one cluster
7:   for  $k = 0: K - 1$  do
8:     The  $m(t)$ th ES broadcasts the most up-to-date global model parameter  $w_k^t$  to all the clients in set  $\mathcal{N}_{m(t)}$ .
9:     for every client  $n \in \mathcal{N}_{m(t)}$  in parallel do
10:      Receive the global parameter  $w_k^t$ . Randomly select dataset  $\xi_{n,k}$  and evaluate  $\nabla f(w_k^t, \xi_{n,k})$ .
11:      Upload  $\nabla f(w_k^t, \xi_{n,k})$  to  $m(t)$ th ES.
12:     end for
13:     The  $m(t)$ th ES receives every  $\nabla f(w_k^t, \xi_{n,k})$  for  $n \in \mathcal{N}_{m(t)}$  and generates  $w_{k+1}^t$  according to Equation (5).
14:   end for
15:   %% The selection of next passing cluster.
16:   The  $m(t)$ th ES retrieves the information of  $D_{A,m}$  and the value of  $c(m)$  from ES node  $m \in \mathcal{A}_{m(t)}$ , and selects the next passing node ES  $m(t+1)$  according to the 2-step operation.
17:   The  $m(t)$ th ES sets  $w_0^{t+1} = w^{t+1} = w_K^t$  and sends the most up-to-date global model parameter  $w_0^{t+1}$  to  $m(t+1)$ th ES.
18:   The  $m(t+1)$ th ES updates  $c(m(t+1)) = c(m(t+1)) + 1$ .
19: end for
20: Output  $w^T$ .

```

4 Theoretical Results

In this section, we theoretically analyze the convergence performance of Fed-CHS over the non-IID datasets. Due to limited space, necessary assumptions are listed in Section F. Then analytical results of convergence on our proposed Fed-CHS are presented based on assumptions. All the proofs are deferred to Appendix G and Appendix H.

4.1 For μ -strongly convex loss function

Theorem 4.1. *With the holding of Assumption F.1, Assumption F.2, Assumption F.3, and Assumption F.4, for the set of η_k such that $\eta_k \leq \frac{1}{2LK}$, $\forall k \in \mathcal{K}$, define*

$$\Delta_m \triangleq \sum_{n \in \mathcal{N}_m} \gamma_n^m (f_n(w^t) - f_n(w^*)); \tau_m \triangleq \sum_{n \in \mathcal{N}_m} \gamma_n^m (f_n(w^*) - f_n^*), \forall m \in \mathcal{M}; \beta \triangleq \frac{\mu}{2} \sum_{k=0}^{K-1} \eta_k, \quad (6)$$

where w^* is the global minimizer of loss function $F(w)$ and f_n^* is the minimum of $f_n(w)$, then there is

$$\begin{aligned} \mathbb{E}\{F(w^T)\} - F(w^*) &\leq \frac{L}{2} (1 - \beta)^T \|w^0 - w^*\|^2 + \frac{L}{2} \sum_{k=0}^{K-1} 6LK\eta_k^2 \sum_{t=0}^{T-1} (1 - \beta)^t \tau_{m(t)} \\ &+ \frac{L}{2} \sum_{k=0}^{K-1} 2\eta_k (1 - 2LK\eta_k) (LK\eta_k - 1) \sum_{t=0}^{T-1} (1 - \beta)^t \Delta_{m(t)} + \frac{L}{2} \sum_{k=0}^{K-1} \frac{2k}{K} \sum_{j=0}^{k-1} \eta_j^2 \sum_{t=0}^{T-1} (1 - \beta)^t G^2 \\ &+ \frac{L}{2} \sum_{k=0}^{K-1} \left(K\eta_k^2 + \frac{2k}{K} \sum_{j=0}^{k-1} \eta_j^2 \right) \sum_{t=0}^{T-1} (1 - \beta)^t \theta_{m(t)}^2 \end{aligned} \quad (7)$$

Proof. See Appendix G. □

Remark 4.2. The bound of optimality gap in Equation (7) reveals the impact of various system parameters on the performance of training model. To reduce the optimality gap, we need to suppress the right-hand side of Equation (7) as much as possible. In the following, discussion is unfolded to show how to make the suppression under some specific configuration of η_k for $k \in \mathcal{K}$.

- Empirically, we do not wish $\{\eta_k\}$ to be too small. Hence we first set η_k as $\eta_k = \frac{1}{2LK\sqrt{k+1}}$, which satisfies $\eta_k < \frac{1}{2LK}$ for $k \in \mathcal{K}$ naturally. In this case, $\beta = \frac{\mu}{2} \sum_{k=0}^{K-1} \eta_k = \frac{\mu}{4L} \sum_{k=0}^{K-1} \frac{1}{K\sqrt{k}} = \mathcal{O}(1/\sqrt{K})$, which can be within $(0, 1)$ as K is large enough. Thus the first term of right-hand side of Equation (7) will trend to be zero at linear rate as T grows. For the rest terms of right-hand side of Equation (7), we notice that $\sum_{t=0}^{T-1} (1-\beta)^t \leq \frac{1}{\beta} = \mathcal{O}(\sqrt{K})$, $\sum_{k=0}^{K-1} \eta_k^2 = \mathcal{O}(\frac{\ln K}{K^2})$, $\sum_{k=0}^{K-1} \frac{k}{K} \sum_{j=0}^{k-1} \eta_j^2 = \mathcal{O}(\frac{\ln K}{K})$, $\sum_{k=0}^{K-1} \eta_k(1-2LK\eta_k)(LK\eta_k-1) < 0$. However, we are still unsure about the sign of $\Delta_{m(t)}$ by inspecting its definition. By assuming $|\Delta_{m(t)}| \leq \Delta_{\max}$, $|\theta_{m(t)}| \leq \theta_{\max}$ and $\tau_{m(t)} \leq \tau_{\max}$, the asymptotic expression of the right-hand side of Equation (7) can be written as $\mathcal{O}\left((1-\beta)^T + \frac{\ln K}{\sqrt{K}}(\theta_{\max}^2 + G^2 + \tau_{\max})\right) + \mu\Delta_{\max}$, which will converge to $\mu\Delta_{\max}$ at linear rate with T and at rate $\mathcal{O}(\ln K/\sqrt{K})$ with K .
- To further speedup convergence rate with K , we explore another way of $\{\eta_k\}$ configuration, which sets $\eta_k = \frac{1}{2LK^q}$ with $q \geq 2$. This set of $\{\eta_k\}$ also fulfills $\eta_k \leq \frac{1}{2LK}$ for $k \in \mathcal{K}$. By following the similar analytical procedure as for previous $\{\eta_k\}$ configuration, the optimality gap can be bounded as $\mathcal{O}\left((1-\beta)^T + \frac{1}{K^{q-1}}\right) + \mu\Delta_{\max}$, which achieves a faster convergence rate with K . This convergence rate is also adjustable by q .
- Note that the optimality gap is not zero because of the existence of $\Delta_{m(t)}$. In this setup, we partly relax the assumption of data heterogeneity. Specifically, we still respect the data heterogeneity among clients within any cluster but assume the data distribution among clusters to be identical. This assumption is still reasonable. To given an instance, for the integrated LEO satellite terrestrial network demonstrated in Section D, every bypassing LEO satellite is an ES node but covers the same group of clients on the ground. Hence the data distribution over clusters is identical and the expectation of $\Delta_{m(t)}$ can be regarded as 0. In this case, with previously suggested setup of $\{\eta_k\}$, zero optimality gap is achieved.

4.2 For non-convex loss function

Theorem 4.3. *With the holding of Assumption F.1 and Assumption F.4, for the set of η_k such that $\eta_k \leq 1/(LK), \forall k \in \mathcal{K}$, there is*

$$\mathbb{E} \left[\frac{1}{T} \sum_{t=0}^{T-1} \|\nabla F(w^t)\|^2 \right] \leq \frac{4[F(w^0) - F(w^*)]}{T \sum_{k=0}^{K-1} \eta_k} + \left(\frac{2LK \sum_{k=0}^{K-1} \eta_k^2}{\sum_{k=0}^{K-1} \eta_k} + 4 \right) \frac{1}{T} \sum_{t=0}^{T-1} \theta_{m(t)}^2 + \frac{2}{T} \sum_{t=0}^{T-1} \sigma^2 \quad (8)$$

Proof. See Appendix H. □

Remark 4.4. The bound in Equation (8) clearly reveals how the sampling variance in one cluster, which is indicated by θ_m^2 for $m \in \mathcal{M}$, and the data heterogeneity among clusters, which is indicated by σ^2 , affect the convergence performance. To achieve a tighter bound, we made the following configurations of $\{\eta_k\}$:

- Like the discussion in Remark 4.2, we first set $\eta_k = 1/(LK\sqrt{k+1})$ for $k \in \mathcal{K}$. In this case, $1/\sum_{k=0}^{K-1} \eta_k = \mathcal{O}(\sqrt{K})$ and $(K \sum_{k=0}^{K-1} \eta_k^2) / \sum_{k=0}^{K-1} \eta_k = \mathcal{O}(\ln K/\sqrt{K})$, then the right-hand side of Equation (8) is upper bounded by

$$\mathcal{O} \left(\frac{\sqrt{K}}{T} (F(w^0) - F(w^*)) + \frac{\ln K}{\sqrt{K}} \sum_{t=0}^{T-1} \theta_{m(t)}^2 \right) + \frac{4}{T} \sum_{t=0}^{T-1} \theta_{m(t)}^2 + 2\sigma^2, \quad (9)$$

which will converge if T grows faster than \sqrt{K} and $\mathcal{O}\left((\sqrt{K}/T)(F(w^0) - F(w^*)) + (\ln K/\sqrt{K}) \sum_{t=0}^{T-1} \theta_{m(t)}^2\right)$ goes to zero with the increase of K .

Table 1: The global model performance of different algorithms on MNIST, CIFAR-10 and CIFAR-100 with $\lambda=0.3$ or $\lambda=0.6$. We set 100 clients, 10 ESS, $T=4000$, $K=20$ and other general settings.

Dataset	Loss Function	Fed-CHS		FEDAVG		WRWGD		Hier-Local-QSGD	
		Dirichlet(0.3)	Dirichlet(0.6)	Dirichlet(0.3)	Dirichlet(0.6)	Dirichlet(0.3)	Dirichlet(0.6)	Dirichlet(0.3)	Dirichlet(0.6)
MNIST	MLP	0.9811	0.9811	0.9813	0.9821	0.9761	0.9767	0.9705	0.9751
	LENET	0.9921	0.9918	0.9912	0.9916	0.9891	0.9888	0.9909	0.9907
CIFAR-10	MLP	0.6249	0.6324	0.5775	0.6380	0.5166	0.5338	0.5685	0.5772
	LENET	0.8198	0.8237	0.7364	0.8042	0.7378	0.7631	0.6805	0.7545
CIFAR-100	MLP	0.3316	0.3322	0.3067	0.3123	0.1950	0.2273	0.2249	0.2636
	LENET	0.4766	0.4790	0.3151	0.3184	0.2920	0.3245	0.3558	0.4021

- To further speedup convergence and express convergence gap in a simple way, we alternatively set $T^{q_1} = K$ and $\eta = 1/(LT^{q_2})$ with $q_1 \in (0, 1)$, $q_2 \geq q_1$, and $1 + q_1 > q_2$. With such a configuration, the right-hand side of Equation (8) is bounded by

$$O\left(\frac{1}{T^{1+q_1-q_2}}(F(w^0) - F(w^*)) + \frac{1}{T^{q_2-q_1}}\sum_{t=0}^{T-1}\theta_{m(t)}^2\right) + \frac{4}{T}\sum_{t=0}^{T-1}\theta_{m(t)}^2 + 2\sigma^2, \quad (10)$$

which converges at a rate $O(1/T^{1+q_1-q_2})$. The convergence rate can be easily adjusted by changing q_1 or q_2 , such that $q_1 \in (0, 1)$, $q_2 \geq q_1$, and $1 + q_1 > q_2$, and will be surely faster than the bound in Equation (9) as T and K grows.

- From Equation (9) and Equation (10), it can be also observed that these bounds will converge to zero as the variance lead by sampling in one cluster (described by θ_m^2 for $m \in \mathcal{M}$) and the data heterogeneity among the clusters (represented by σ^2) vanish. Hence stationary point is reached.

5 Experiments

Several important experimental results are presented in this section, whose detailed discussions are postponed to Appendix B and Appendix C.

5.1 Setup

Datasets and Models: We experiment with three datasets, MNIST, CIFAR-10 and CIFAR-100 using the LENET (LeCun et al., 1998, 2015) and Multi-Layer Perceptron (MLP) (Yue et al., 2022) models. The details for datasets are present in Appendix A. The non-IID settings adopted by us involve Dirichlet(λ): the label distribution on each device follows the Dirichlet distribution with $\lambda > 0$ being a concentration parameter. A larger value of λ indicates a more homogeneous distribution across each dataset. The loss function in LENET model and MLP model can be regarded as non-convex and convex, respectively. More details can be found in Appendix A.

Baselines: To empirically highlight the training performance of our proposed framework, we first compare it in the general settings with FedAvg (McMahan et al., 2017), Weighted RWGD (WRWGD) (Ayache and El Rouayheb, 2019), Hier-Local-QSGD (Liu et al., 2023a) based on MNIST, CIFAR-10 and CIFAR-100 datasets. Then, in order to evaluate the communication overhead, we compare our proposed framework in the similar settings with FedAvg compressed by QSGD (Alistarh et al., 2017) and Hier-Local-QSGD based on MNIST, CIFAR-10 datasets for LENET model.

Metrics: To investigate the performance of Fed-CHS, we compare it with other algorithms by measuring the accuracy in the test. A higher test accuracy means that the performance of the associated algorithm is better. During the training process, we also evaluate the communication overhead for passing model parameters. Specifically, we compare the total communication cost for passing model parameters under different algorithms to reach specific threshold of test accuracy, denoted as Γ . For MNIST, CIFAR-10 and CIFAR-100 dataset, Γ is selected to be 0.98, 0.72, 0.40, respectively, by referring to achievable test accuracy in Table 1.

5.2 Results for Training Performance

The experimental results are reported in Table 1. These results show that Fed-CHS can achieve higher accuracy under the majority of configurations, although it may not be consistently superior to

other algorithms. Particularly noteworthy is our proposed Fed-CHS expands its advantage over other baseline algorithms when the data distribution becomes more heterogeneous.

For the easy datasets (MNIST), Fed-CHS is not always the best but only has a tiny performance gap compared with FedAvg, which achieves highest accuracy in this case. It is worthy to note that MNIST dataset has limited number of target classes, which can drive every testing algorithm to perform well easily. Hence some slight disadvantage on MNIST for Fed-CHS does not mean it is inferior to other baselines. For the MLP model on the CIFAR-10 or CIFAR-100 datasets, each algorithm performs poorly, especially for WRWGD and Hier-Local-QSGD. This explains the relatively low level of test accuracy for all the testing algorithms. The above situation alleviates a lot for LeNet model, except of FedAvg on CIFAR-100 dataset.

Additionally, to highlight the stability of our algorithm, the performance of Fed-CHS and other algorithms in different settings where clients use different models and Dirichlet parameters under the datasets of CIFAR10, CIFAR100, and MNIST is plotted with round number T , as given in Appendix C. An improvement of accuracy over baselines ranges from 0.02% and 33.95% can be observed. Further analysis can be also found from Appendix C.

5.3 Results for Communication Overhead

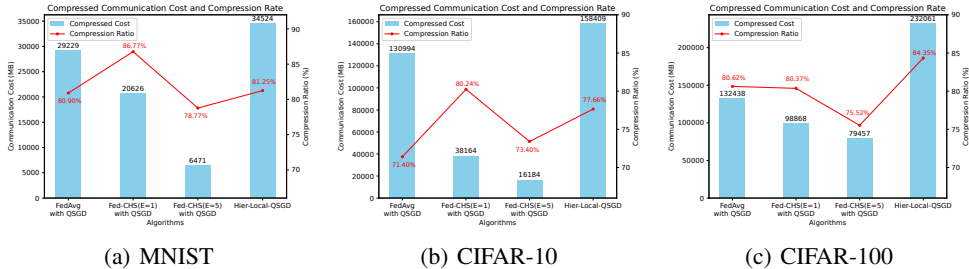


Figure 2: Results of communication overhead for different algorithms and datasets.

We recorded the total communication overhead (in unit of information bits) of our algorithm and the baselines to achieve default Γ with compression, and the percentage reduction in communication overhead with the aid of compression, in Figure 2. Therefore the communication overhead without compression can be also inferred from Figure 2. Notably, for Fed-CHS, a total number of aggregations within one cluster is 20. Hence every client interacts with associated ES by 20 times when $E = 1$, which will turn to be 4 times when $E = 5$. It is evident that for datasets MNIST, CIFAR-10, or CIFAR-100, our algorithm significantly outperforms other baseline algorithms in terms of total communication overhead with or without compression. This result is reasonable because the passing of aggregated model parameter among ESs, rather than further aggregating them at a PS, can help to save a lot of communication overhead compared with FedAvg (with QSGD) or Hier-Local-QSGD, and does not degrade the convergence performance too much. There is one more thing to highlight, the counted communication for Fed-CHS happens between a client and an associated ES or an ES and its neighbor ES, all of which only involve one-hop communication, while the counted communication between a client and the PS in FedAvg (with QSGD) may be over a long distance that will ask for multiple hops of routing and incur heavier communication burden.

6 Conclusion

In this paper, we propose a new federated learning algorithm Fed-CHS, which introduces SFL into HFL for the first time to further reduce communication overhead for passing model parameters. Theoretical analysis guarantees the convergence performance of the Fed-CHS for strongly convex or non-convex loss function under various setup of data heterogeneity. Extensive experiments are conducted to verify the advantage of our proposed Fed-CHS in terms of test accuracy, communication overhead saving, and convergence over existing methods. In the future, we will extend our theoretical analysis from the setup of single-step local iteration to multi-step, which is more general. And the potential of this setup has been verified in existing experiments on communication overhead.

References

- Abad, M. S. H., Ozfatura, E., GÜndüz, D., and Ercetin, O. (2020). Hierarchical federated learning across heterogeneous cellular networks. In *ICASSP 2020 - 2020 IEEE International Conference on Acoustics, Speech and Signal Processing*, pages 8866–8870.
- Alistarh, D., Grubic, D., Li, J., Tomioka, R., and Vojnovic, M. (2017). Qsgd: Communication-efficient sgd via gradient quantization and encoding. In *Advances in Neural Information Processing Systems*, volume 30. Curran Associates, Inc.
- Amiri, M. M. and Gündüz, D. (2020). Federated learning over wireless fading channels. *IEEE Transactions on Wireless Communications*, 19(5):3546–3557.
- Ayache, G., Dassari, V., and Rouayheb, S. E. (2023). Walk for learning: A random walk approach for federated learning from heterogeneous data. *IEEE Journal on Selected Areas in Communications*, 41(4):929–940.
- Ayache, G. and El Rouayheb, S. (2019). Random walk gradient descent for decentralized learning on graphs. In *2019 IEEE International Parallel and Distributed Processing Symposium Workshops*, pages 926–931.
- Bibikar, S., Vikalo, H., Wang, Z., and Chen, X. (2022). Federated dynamic sparse training: Computing less, communicating less, yet learning better. *Proceedings of the AAAI Conference on Artificial Intelligence*, 36(6):6080–6088.
- Briggs, C., Fan, Z., and Andras, P. (2020). Federated learning with hierarchical clustering of local updates to improve training on non-iid data. In *2020 International Joint Conference on Neural Networks*, pages 1–9.
- Collins, L., Hassani, H., Mokhtari, A., and Shakkottai, S. (2022). Fedavg with fine tuning: Local updates lead to representation learning. In *Advances in Neural Information Processing Systems*, volume 35, pages 10572–10586.
- Das, R., Acharya, A., Hashemi, A., Sanghavi, S., Dhillon, I. S., and Topcu, U. (2022). Faster non-convex federated learning via global and local momentum. In *Proceedings of the Thirty-Eighth Conference on Uncertainty in Artificial Intelligence*, volume 180, pages 496–506. PMLR.
- Deng, Y., Lyu, F., Ren, J., Zhang, Y., Zhou, Y., Zhang, Y., and Yang, Y. (2021). Share: Shaping data distribution at edge for communication-efficient hierarchical federated learning. In *2021 IEEE 41st International Conference on Distributed Computing Systems*, pages 24–34.
- Gu, X., Huang, K., Zhang, J., and Huang, L. (2021). Fast federated learning in the presence of arbitrary device unavailability. In *Advances in Neural Information Processing Systems*, volume 34, pages 12052–12064.
- Horváth, S., Laskaridis, S., Almeida, M., Leontiadis, I., Venieris, S., and Lane, N. (2021). Fjord: Fair and accurate federated learning under heterogeneous targets with ordered dropout. In *Advances in Neural Information Processing Systems*, volume 34, pages 12876–12889.
- Hosseinalipour, S., Azam, S. S., Brinton, C. G., Michelusi, N., Aggarwal, V., Love, D. J., and Dai, H. (2022). Multi-stage hybrid federated learning over large-scale d2d-enabled fog networks. *IEEE/ACM Transactions on Networking*, 30(4):1569–1584.
- Huang, M., Zhang, D., and Ji, K. (2023). Achieving linear speedup in non-iid federated bilevel learning. *arXiv preprint arXiv:2302.05412*.
- Jhunjhunwala, D., Sharma, P., Nagarkatti, A., and Joshi, G. (2022). Fedvarp: Tackling the variance due to partial client participation in federated learning. In *Proceedings of the Thirty-Eighth Conference on Uncertainty in Artificial Intelligence*, volume 180, pages 906–916. PMLR.
- Karimireddy, S. P., Kale, S., Mohri, M., Reddi, S., Stich, S., and Suresh, A. T. (2020). Scaffold: Stochastic controlled averaging for federated learning. In *International conference on machine learning*, volume 119, pages 5132–5143. PMLR.

- Khaled, A., Mishchenko, K., and Richtárik, P. (2020). Tighter theory for local sgd on identical and heterogeneous data. In *International Conference on Artificial Intelligence and Statistics*, volume 108, pages 4519–4529. PMLR.
- Koloskova, A., Stich, S. U., and Jaggi, M. (2022). Sharper convergence guarantees for asynchronous sgd for distributed and federated learning. In *Advances in Neural Information Processing Systems*, volume 35, pages 17202–17215.
- LeCun, Y., Bottou, L., Bengio, Y., and Haffner, P. (1998). Gradient-based learning applied to document recognition. *Proceedings of the IEEE*, 86(11):2278–2324.
- LeCun, Y. et al. (2015). Lenet-5, convolutional neural networks. URL: <http://yann.lecun.com/exdb/lenet>, 20(5):14.
- Letaief, K. B., Shi, Y., Lu, J., and Lu, J. (2022). Edge artificial intelligence for 6g: Vision, enabling technologies, and applications. *IEEE Journal on Selected Areas in Communications*, 40(1):5–36.
- Li, Q., Diao, Y., Chen, Q., and He, B. (2022). Federated learning on non-iid data silos: An experimental study. In *2022 IEEE 38th International Conference on Data Engineering*, pages 965–978.
- Li, X., Huang, K., Yang, W., Wang, S., and Zhang, Z. (2020). On the convergence of fedavg on non-iid data. In *International Conference on Learning Representations*.
- Li, X. and Li, P. (2023). Analysis of error feedback in federated non-convex optimization with biased compression: Fast convergence and partial participation. In *Proceedings of the 40th International Conference on Machine Learning*, volume 202, pages 19638–19688. PMLR.
- Lim, W. Y. B., Ng, J. S., Xiong, Z., Jin, J., Zhang, Y., Niyato, D., Leung, C., and Miao, C. (2022). Decentralized edge intelligence: A dynamic resource allocation framework for hierarchical federated learning. *IEEE Transactions on Parallel and Distributed Systems*, 33(3):536–550.
- Liu, L., Zhang, J., Song, S., and Letaief, K. B. (2020). Client-edge-cloud hierarchical federated learning. In *ICC 2020 - 2020 IEEE International Conference on Communications*, pages 1–6.
- Liu, L., Zhang, J., Song, S., and Letaief, K. B. (2023a). Hierarchical federated learning with quantization: Convergence analysis and system design. *IEEE Transactions on Wireless Communications*, 22(1):2–18.
- Liu, X., Wang, Q., Shao, Y., and Li, Y. (2023b). Sparse federated learning with hierarchical personalization models. *IEEE Internet of Things Journal*, pages 1–1.
- Lu, Y., Huang, X., Zhang, K., Maharjan, S., and Zhang, Y. (2020). Blockchain empowered asynchronous federated learning for secure data sharing in internet of vehicles. *IEEE Transactions on Vehicular Technology*, 69(4):4298–4311.
- Luo, B., Li, X., Wang, S., Huang, J., and Tassiulas, L. (2021). Cost-effective federated learning design. In *IEEE INFOCOM 2021 - IEEE Conference on Computer Communications*, pages 1–10.
- Luo, B., Xiao, W., Wang, S., Huang, J., and Tassiulas, L. (2022). Tackling system and statistical heterogeneity for federated learning with adaptive client sampling. In *IEEE INFOCOM 2022 - IEEE Conference on Computer Communications*, pages 1739–1748.
- Ma, X., Zhu, J., Lin, Z., Chen, S., and Qin, Y. (2022). A state-of-the-art survey on solving non-iid data in federated learning. *Future Generation Computer Systems*, 135:244–258.
- Mao, X., Yuan, K., Hu, Y., Gu, Y., Sayed, A. H., and Yin, W. (2020). Walkman: A communication-efficient random-walk algorithm for decentralized optimization. *IEEE Transactions on Signal Processing*, 68:2513–2528.
- Martínez Beltrán, E. T., Pérez, M. Q., Sánchez, P. M. S., Bernal, S. L., Bovet, G., Pérez, M. G., Pérez, G. M., and Celdrán, A. H. (2023). Decentralized federated learning: Fundamentals, state of the art, frameworks, trends, and challenges. *IEEE Communications Surveys & Tutorials*, 25(4):2983–3013.

- McMahan, B., Moore, E., Ramage, D., Hampson, S., and Arcas, B. A. y. (2017). Communication-efficient learning of deep networks from decentralized data. In *Proceedings of the 20th International Conference on Artificial Intelligence and Statistics*, volume 54, pages 1273–1282. PMLR.
- Ng, J. S., Lim, W. Y. B., Xiong, Z., Cao, X., Jin, J., Niyato, D., Leung, C., and Miao, C. (2022). Reputation-aware hedonic coalition formation for efficient serverless hierarchical federated learning. *IEEE Transactions on Parallel and Distributed Systems*, 33(11):2675–2686.
- Nguyen, D. C., Hosseinalipour, S., Love, D. J., Pathirana, P. N., and Brinton, C. G. (2022). Latency optimization for blockchain-empowered federated learning in multi-server edge computing. *IEEE Journal on Selected Areas in Communications*, 40(12):3373–3390.
- Parsons, Z., Dou, F., Du, H., Song, Z., and Lu, J. (2023). Mobilizing personalized federated learning in infrastructure-less and heterogeneous environments via random walk stochastic admm. In Oh, A., Naumann, T., Globerson, A., Saenko, K., Hardt, M., and Levine, S., editors, *Advances in Neural Information Processing Systems*, volume 36, pages 36726–36737. Curran Associates, Inc.
- Pham, Q.-V., Zeng, M., Huynh-The, T., Han, Z., and Hwang, W.-J. (2022). Aerial access networks for federated learning: Applications and challenges. *IEEE Network*, 36(3):159–166.
- Qu, Z., Duan, R., Chen, L., Xu, J., Lu, Z., and Liu, Y. (2022). Context-aware online client selection for hierarchical federated learning. *IEEE Transactions on Parallel and Distributed Systems*, 33(12):4353–4367.
- Rothchild, D., Panda, A., Ullah, E., Ivkin, N., Stoica, I., Braverman, V., Gonzalez, J., and Arora, R. (2020). FetchSGD: Communication-efficient federated learning with sketching. In *Proceedings of the 37th International Conference on Machine Learning*, volume 119, pages 8253–8265. PMLR.
- Shah, S. M. and Lau, V. K. N. (2023). Model compression for communication efficient federated learning. *IEEE Transactions on Neural Networks and Learning Systems*, 34(9):5937–5951.
- Shi, L., Shu, J., Zhang, W., and Liu, Y. (2021). Hfl-dp: Hierarchical federated learning with differential privacy. In *2021 IEEE Global Communications Conference (GLOBECOM)*, pages 1–7.
- Song, B., Khanduri, P., Zhang, X., Yi, J., and Hong, M. (2023). FedAvg converges to zero training loss linearly for overparameterized multi-layer neural networks. In *Proceedings of the 40th International Conference on Machine Learning*, volume 202, pages 32304–32330. PMLR.
- Sun, T., Li, D., and Wang, B. (2022). Adaptive random walk gradient descent for decentralized optimization. In *Proceedings of the 39th International Conference on Machine Learning*, volume 162, pages 20790–20809. PMLR.
- Tu, Y., Ruan, Y., Wagle, S., Brinton, C. G., and Joe-Wong, C. (2020). Network-aware optimization of distributed learning for fog computing. In *IEEE INFOCOM 2020-IEEE Conference on Computer Communications*, pages 2509–2518. IEEE.
- WANG, L., WANG, W., and LI, B. (2019). Cmf1: Mitigating communication overhead for federated learning. In *2019 IEEE 39th International Conference on Distributed Computing Systems*, pages 954–964.
- Wang, S., Tuor, T., Salonidis, T., Leung, K. K., Makaya, C., He, T., and Chan, K. (2019). Adaptive federated learning in resource constrained edge computing systems. *IEEE Journal on Selected Areas in Communications*, 37(6):1205–1221.
- Wang, Z., Hu, Y., Yan, S., Wang, Z., Hou, R., and Wu, C. (2022). Efficient ring-topology decentralized federated learning with deep generative models for medical data in healthcare systems. *Electronics*, 11(10):1548.
- Wang, Z., Xu, H., Liu, J., Huang, H., Qiao, C., and Zhao, Y. (2021). Resource-efficient federated learning with hierarchical aggregation in edge computing. In *IEEE INFOCOM 2021 - IEEE Conference on Computer Communications*, pages 1–10.
- Wang, Z., Xu, H., Liu, J., Xu, Y., Huang, H., and Zhao, Y. (2023). Accelerating federated learning with cluster construction and hierarchical aggregation. *IEEE Transactions on Mobile Computing*, 22(7):3805–3822.

- Xiao, P. and Ji, K. (2023). Communication-efficient federated hypergradient computation via aggregated iterative differentiation. *arXiv preprint arXiv:2302.04969*.
- Xu, H., Han, S., Li, X., and Han, Z. (2023). Anomaly traffic detection based on communication-efficient federated learning in space-air-ground integration network. *IEEE Transactions on Wireless Communications*, 22(12):9346–9360.
- Yang, H. (2021). H-fl: A hierarchical communication-efficient and privacy-protected architecture for federated learning. *arXiv preprint arXiv:2106.00275*.
- You, C., Guo, K., Yang, H. H., and Quek, T. Q. S. (2023). Hierarchical personalized federated learning over massive mobile edge computing networks. *IEEE Transactions on Wireless Communications*, 22(11):8141–8157.
- Yue, K., Jin, R., Pilgrim, R., Wong, C.-W., Baron, D., and Dai, H. (2022). Neural tangent kernel empowered federated learning. In *Proceedings of the 39th International Conference on Machine Learning*, volume 162, pages 25783–25803. PMLR.
- Zaccone, R., Rizzardi, A., Caldarola, D., Ciccone, M., and Caputo, B. (2022). Speeding up heterogeneous federated learning with sequentially trained superclients. In *2022 26th International Conference on Pattern Recognition*, pages 3376–3382.
- Zhang, H., Liu, J., Jia, J., Zhou, Y., Dai, H., and Dou, D. (2022). Fedduap: Federated learning with dynamic update and adaptive pruning using shared data on the server. In *Proceedings of the Thirty-First International Joint Conference on Artificial Intelligence, IJCAI-22*, pages 2776–2782.
- Zhang, Z., Li, Y., Huang, C., Guo, Q., Liu, L., Yuen, C., and Guan, Y. L. (2020). User activity detection and channel estimation for grant-free random access in leo satellite-enabled internet of things. *IEEE Internet of Things Journal*, 7(9):8811–8825.
- Zhao, M., Chen, C., Liu, L., Lan, D., and Wan, S. (2022). Orbital collaborative learning in 6g space-air-ground integrated networks. *Neurocomputing*, 497:94–109.
- Zhou, Y., Shi, Y., Zhou, H., Wang, J., Fu, L., and Yang, Y. (2023). Toward scalable wireless federated learning: Challenges and solutions. *IEEE Internet of Things Magazine*, 6(4):10–16.

Contents

1	Introduction	1
2	Related Work in Brief	3
3	Fed-CHS	3
3.1	Problem Setup	4
3.2	Algorithm Description	5
4	Theoretical Results	6
4.1	For μ -strongly convex loss function	6
4.2	For non-convex loss function	7
5	Experiments	8
5.1	Setup	8
5.2	Results for Training Performance	8
5.3	Results for Communication Overhead	9
6	Conclusion	9
A	Implementation Details	16
B	Issues about Hyper-parameters	16
B.1	Hyper-parameter Settings	16
B.2	Results for Impact of Hyper-parameters	17
C	Additional Comparison Results for Training Performance	18
D	Application Scenarios of SFL in Hierarchical Architecture	19
E	Related Work in Detail	20
F	Assumptions	20
G	Proof of Theorem Theorem 4.1	21
G.1	Key Lemmas	21
G.2	Completing the Proof of Theorem 4.1	22
H	Proof of Theorem Theorem 4.3	25
H.1	Key Lemmas	25
H.2	Completing the Proof of Theorem 4.3	25
I	Defered Proof of Lemmas	27
I.1	Proof of Lemma G.1	27

I.2	Proof of Lemma G.2	28
I.3	Proof of Lemma G.3	30
I.4	Proof of Lemma H.1	31
I.5	Proof of Lemma H.2	31

A Implementation Details

We experiment with three datasets, MNIST, CIFAR-10 and CIFAR-100 using the LENET (LeCun et al., 1998, 2015) and Multi-Layer Perceptron (MLP) (Yue et al., 2022) models. Firstly, we describe the datasets as below:

- **MNIST:** It contains 60000 train samples and 10000 test samples. Each sample is a 28×28 scale image associated with a label from 10 classes.
- **CIFAR-10:** It is a dataset that includes 10 different types of color images, with 6000 images in each category, totaling 60000 images. All images are divided into 50000 train samples and 10000 test samples. Each image has a resolution of 32×32 pixels and includes 3 color channels (RGB).
- **CIFAR-100:** It includes 50000 train samples and 10000 test samples, each associated with 100 possible labels. The sample in CIFAR-100 is a 32×32 color image.

The non-IID settings we adopt involve Dirichlet(λ): the label distribution on each device follows the Dirichlet distribution, where λ is a concentration parameter ($\lambda > 0$). A larger value of λ indicates a more homogeneous distribution across each dataset. The loss function in LENET model is non-convex and the loss function in MLP model is convex. Next, we represent the network model used in experiments as below:

- **MLP:** There are two fully connected layers in MLP, apart from the input layer and the output layer. For MNIST, these two fully connected layers both have 200 neurons. For CIFAR-10 and CIFAR-100, the amount of neurons in the two fully connected layers is 256 and 512, respectively. We all set ReLU as the activation function of the two middle layers.
- **LENET:** Different from the MLP, we add two sets of concatenated convolution layer and pooling layer between the input layer and the fully connected layer in LENET. For these two convolution layers, we utilize 64 and 256 convolution kernels to train MNIST respectively, each with a size of 5×5 . And we utilize two 64 convolution kernels having been adopted for MNIST to train CIFAR-10 and CIFAR-100 respectively. Additionally, all the pooling layers are set to be 2×2 . In case of MNIST dataset, there are two fully connected layers with dimensions 512×512 and 128×128 , respectively. For CIFAR-10 and CIFAR-100 datasets, the two fully connected layers have dimensions of 384×384 and 192×192 .

To carry out our experiments, we set up a machine learning environments in PyTorch 2.2.2 on Ubuntu 20.04, powered by four RTX A6000 GPUs and AMD 7702 CPU.

B Issues about Hyper-parameters

B.1 Hyper-parameter Settings

In this work, we generally employed 100 devices to simulate a substantial number of participating clients in practical FL. For the hierarchical architecture, we set 10 ES's with each ES being assigned with some clients. All clients are selected to generate the global model. For non-IID settings of the datasets, the parameter λ of Dirichlet needs to be set, we use $\lambda = 0.6$ generally and we also use the setting group with $\lambda = 0.3$ and $\lambda = 0.6$.

Furthermore, we ran these algorithms in $T = 4000$ rounds. In Fed-CHS and Hier-Local-QSGD, the local communication round number within ESs is $K = T^{q_1} = 20$ and the value of the learning rate is set as $\frac{1}{K\sqrt{k+1}}$ in the k -th communication. And for FedAvg and Weighted RWGD, we set the training epochs in clients to be $K = 20$ and the value of the learning rate as $\frac{1}{K\sqrt{k+1}} = \frac{1}{LT^{q_2}}$ in the k -th communication. For Fed-CHS and Weighted RWGD, we first randomly generate the network topology before these algorithms begin to train. The ES (or client) node is required to be connected with at most three other ES (or client) nodes for the network topology of Fed-CHS (or Weighted RWGD), which uses a relatively sparse connection approach to better mimic the physical connectivity. To evaluate the total communication cost, we represent each parameter by 32 bits. For ease of comparison, in Fed-CHS and FedAvg, each client performs one local iteration per round, while in Hier-Local-QSGD, each client performs 5 local iterations per round. Both Fed-CHS and Hier-Local-QSGD conduct 20 iterations per round within the cluster.

B.2 Results for Impact of Hyper-parameters

In this subsection, we examine the impact of the number of local communication rounds, the degree of data heterogeneity and the number of ES's on our proposed Fed-CHS. Additionally, we also examine the impact of partial data heterogeneity within one cluster on Fed-CHS.

Figure 3(a) and Figure 3(d) show that our Fed-CHS's convergence rate varies with the number of local communication rounds. In case a smaller K is adopted, which implies a higher learning rate, a faster convergence rate can be achieved. According to Theorem 4.3, the gap of convergence is weakly affected by K , the influence of which is even weaker as T grows. This explains the fact that the training accuracy trends to be similar as T increases. Both Figure 3(b) and Figure 3(e) reveal that severe data heterogeneity may exert influence on the training accuracy significantly. But as the dataset distributions among clients tend to be more homogeneous, this kind of influence is likely to decay. As a comparison, the difference of training accuracy due to data homogeneity is more sensitive to convex loss function, like in MLP, rather than a non-convex loss function, like in LENET. Figure 3(c) and Figure 3(f) clearly illustrate that too many ES's may lead to a bad performance. The reason can be explained as follows: With the population of clients unchanged but the number of ES's increased, each ES shares a less fraction of clients, which leads to a less generality of the locally trained model within one cluster. Sequential updating of this kind of model among clusters become a repetitive correcting process of the model only being adapt to the dataset of the clients in currently active cluster, rather than an evolving process of the model that can represent the global data distribution of all the clients.

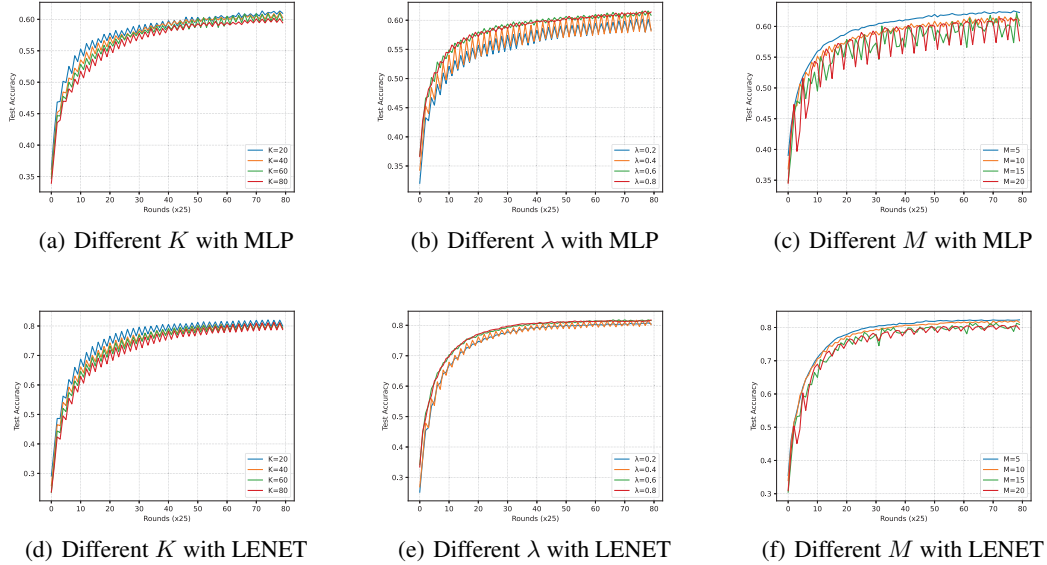


Figure 3: Results for different hyper-parameters with MLP or LENET

We also inspect the training performance of Fed-CHS under fully or partially heterogeneous dataset by using LENET model and CIFAR-10 dataset in Figure 4. When partial data heterogeneity is implemented, the dataset distribution among clusters are IID but the dataset distribution among clients within any cluster is non-IID. The extent of heterogeneity is still tuned by parameter λ . As of training performance, both test accuracy and training loss are probed. From Figure 4, we observe that the performance gap due to the difference between fully and partially heterogeneous datasets trends to be diminish as T grows. Also considering the remark in Remark 4.4, we can achieve stationary point for non-convex loss function like the LENET model with partially heterogeneous dataset. Then it can be inferred that the performance of Fed-CHS for training a non-convex loss function under fully heterogeneous dataset can be also promised.

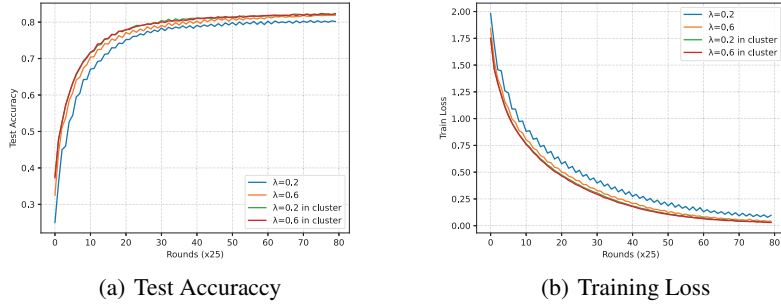


Figure 4: Result for different data heterogeneity in ES

C Additional Comparison Results for Training Performance

Figure 5, Figure 6, and Figure 7 represent the performance of Fed-CHS and other algorithms in different settings where clients use different models and Dirichlet parameters under MNIST, CIFAR-10, and CIFAR-100 dataset, respectively. For Figure 5, all algorithms can achieve good performance, but only Fed-CHS has a stable volatility. In Figure 6, due to the non-IID dataset or the convexity of loss function, which is used to approximate the idea model that is surely non-convex, all the algorithms suffer from different degrees of volatility. Although Fed-CHS doesn't perform the best in convex settings, its performance gap to the optimal one among baseline methods shrinks from 0.1% to 0.02% as data heterogeneity increases. Fed-CHS performs better on volatility and converges faster than all the other algorithms under various settings. From Figure 7, it can be seen that Fed-CHS still outperforms its counterparts not only on volatility but also on convergence speed under LENET model. For MLP model, Fed-CHS exhibits slightly less fluctuation and lower convergence speed compared to FedAvg, but its overall model performance surpasses that of all other baseline methods by a significant margin. The above results prove the advantage of our proposed Fed-CHS.

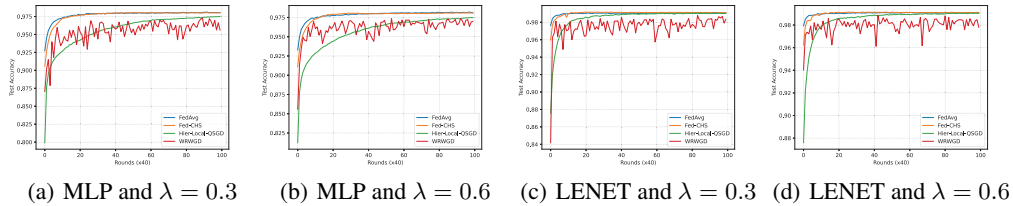


Figure 5: Convergence performance of Fed-CHS and baselines in different models and Dirichlet parameters, using MNIST dataset

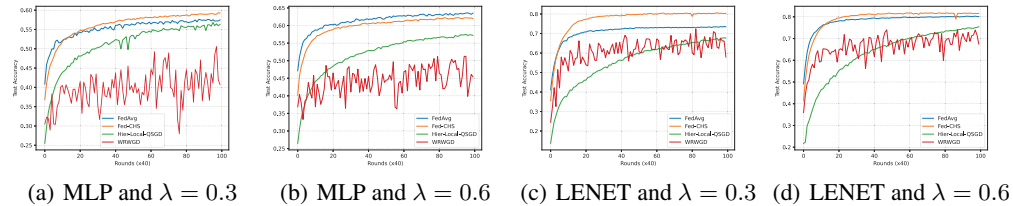


Figure 6: Convergence performance of Fed-CHS and baselines in different models and Dirichlet parameters, using CIFAR-10 dataset

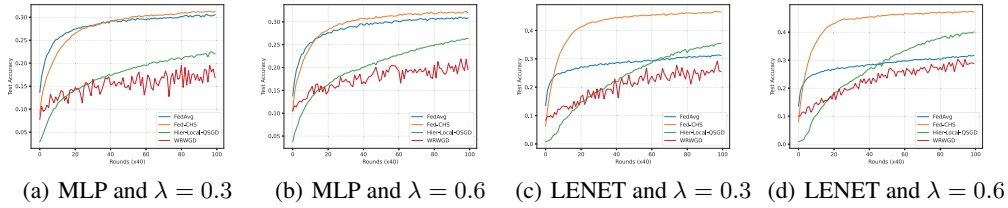


Figure 7: Convergence performance of Fed-CHS and baselines in different models and Dirichlet parameters, using CIFAR-100 dataset

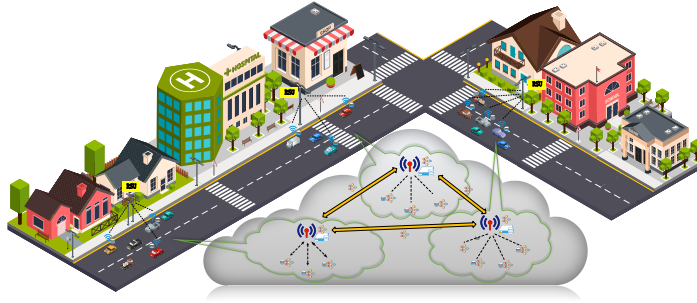


Figure 8: Federated learning used in the scenario of IoV under the combinational framework of HFL and SFL

D Application Scenarios of SFL in Hierarchical Architecture

Internet of Vehicles (IoV): To learn a common model from the vehicles in an IoV by FL, a lot of scattered road side units (RSUs) can be leveraged to aggregate the local model parameter of bypassing vehicles through one-hop wireless link (Lu et al., 2020). In the combinational framework of HFL and SFL, every RSU acts as the ES and the bypassing vehicles are participating clients. Once get the aggregated local model from bypassing vehicles, one RSU can push it to the neighbor RSU for next round of iteration. Through this operation, no data transmission is required from neither any vehicle nor a RSU to a central PS round by round. Lost of traffic burden is saved in the hybrid framework of HFL and SFL. An illustrative figure of this scenario is given in Figure 8 ¹.

Integrated Low-earth Orbit (LEO) Satellite-Terrestrial Network: Integrated LEO satellite-terrestrial network can provide seamless and reliable content delivery service for the users widely distributed on earth’s surface. This type of network such as StarLink has been put into use (Zhao et al., 2022; Xu et al., 2023). To learn a common model from the surface users in a certain area via the FL technique, local model parameters of multiple surface users can be uploaded to the LEO satellite overhead for aggregation (Zhang et al., 2020; Letaief et al., 2022). Restricted by orbit dynamics, every LEO satellite flies over the sky quickly and would not be able to offer the service of parameter aggregation and broadcasting for long. To overcome this challenge, we can adopt the combinational framework of HFL and SFL, in which every LEO satellite above the horizon can be taken as one ES and the surface users correspond to participating clients. Within such a framework, the LEO satellite with the most up-to-date model parameter but has to go below the horizon soon can hand over its model parameter to the LEO satellite arising in the sky. Through this way, parameter aggregation and broadcasting can be sustained round by round between the surface users and the LEO satellites over the sky. This application scenario is demonstrated in Figure 9.

¹Thanks for the courtesy of Freepik.com, which offers parts of the elements for Figure 8 and Figure 9.

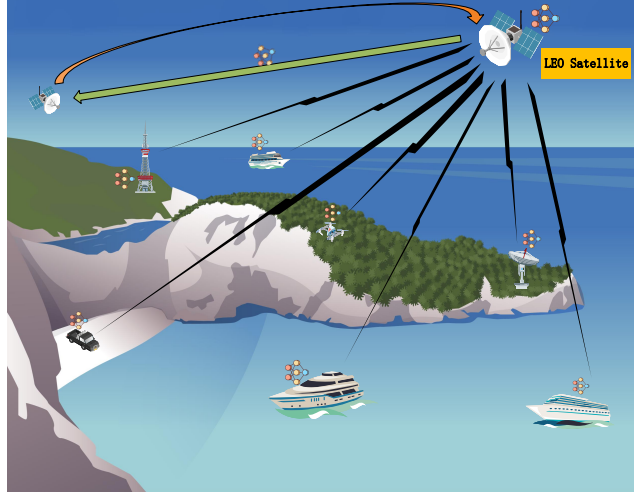


Figure 9: Federated learning under the combinational framework of HFL and SFL for LEO satellite-terrestrial network

E Related Work in Detail

For the literature in HFL, Wang et al. (2023) proposes to update the aggregated model parameter at each ES to the PS asynchronously, which allows the ES currently having bad link condition with the PS to offload its model parameter only when the link condition turns to be good. Tu et al. (2020) leverages fog computing to help the participating clients with weak computation capability. Specifically, when one client cannot update its model parameter at local in time, it can offload its computation task to its neighbor client. Hosseinalipour et al. (2022) builds a multiple-layer (more than two) architecture to cover each participating client in a device-to-device (D2D) enabled network.

In terms of the literature in SFL, when the next passing node is selected in fixed order, Wang et al. (2022) arranges all the participating clients to be in a ring topology. Differently, Zaccone et al. (2022) divides the whole sets of clients into multiple sub-groups, each of which gathers the clients with similar dataset distribution and arranges its clients to be in a ring topology. Global model parameter is firstly updated in sequence among the clients in one sub-group and then pushed to the other sub-group. When the next passing node is selected randomly, Ayache and El Rouayheb (2019) values the neighbor clients, each of which can serve as the candidate of next passing node, with a probability based on the associated Lipschitz constant, which characterizes the smoothness of the local loss function. Mao et al. (2020) maps the gradient of each next passing node candidate’s local loss function to a selecting probability in a straightforward way, while Ayache et al. (2023) makes this mapping by leveraging MAB theory.

As of overcoming data heterogeneity, for conventional FL, when the loss function is strongly convex, Khaled et al. (2020) can promise convergence, while Li et al. (2020) is able to further achieve zero optimality gap. The convergence speed is mainly at $\mathcal{O}(1/T)$ Li et al. (2020) or $\mathcal{O}(1/\sqrt{T})$ Khaled et al. (2020), where T is the number of communication round. For non-convex and smooth loss functions, prior works can ensure convergence Koloskova et al. (2022); Jhunjunwala et al. (2022); Das et al. (2022); Karimireddy et al. (2020) but can hardly achieve stationary point. The convergence rate is mainly at $\mathcal{O}(1/T)$ (Jhunjunwala et al., 2022), $\mathcal{O}(1/T^{\frac{2}{3}})$ (Das et al., 2022), or $\mathcal{O}(1/\sqrt{T})$ (Koloskova et al., 2022; Karimireddy et al., 2020).

F Assumptions

First we state some general assumptions in the work.

Assumption F.1. (L -smooth). The loss function $f(w, z_{n,i})$ is L -smooth if

$$f(w_1, z_{n,i}) \leq f(w_2, z_{n,i}) + \langle \nabla f(w_2, z_{n,i}), w_1 - w_2 \rangle + \frac{L}{2} \|w_1 - w_2\|^2 \quad (11)$$

With Assumption F.1, it can be derived that $f_n(w)$, i.e., the local loss function of n th client, is also L -smooth as they are the linear combination of the L -smooth functions $f(w, z_{n,i})$ for $z_{n,i} \in \mathcal{D}_n$ (Xiao and Ji, 2023). Similarly, the function $F_m(w) \triangleq \sum_{n \in \mathcal{N}_m} \gamma_n^m f_n(w)$ and $F(w)$ are all L -smooth.

Assumption F.2. (μ -strongly Convex). The loss function $f(w, z_{n,i})$ is μ -strongly convex if

$$f(w_1, z_{n,i}) \geq f(w_2, z_{n,i}) + \langle \nabla f(w_2, z_{n,i}), w_1 - w_2 \rangle + \frac{\mu}{2} \|w_1 - w_2\|^2 \quad (12)$$

With Assumption F.2, similar with the discussion after Assumption F.1, $f_n(w)$, $F_m(w)$, and $F(w)$ are all μ -strongly convex as they are the linear combinations of $f(w, z_{n,i})$ for $z_{n,i} \in \mathcal{D}_n$ and $n \in \mathcal{N}$ (Huang et al., 2023; Xiao and Ji, 2023).

Assumption F.3. (Bounded Stochastic Gradient). The norm of gradients is uniformly bounded, i.e.,

$$\|\nabla f_n(w)\|^2 \leq G^2, \forall n \in \mathcal{N} \quad (13)$$

This assumption is general and has been adopted in Koloskova et al. (2022); Li and Li (2023); You et al. (2023). With Assumption F.3, it can be derived from Jensen inequality that $\|\nabla F_m(w)\|^2$ and $\|\nabla F(w)\|^2$ are all upper bounded by G^2 , where $\nabla F_m(w)$ is the gradient of $F_m(w)$ with w .

Assumption F.4. (Bounded Variance and Heterogeneity). For $f_n(w)$ and $f(w, z_{n,i})$, the variance of stochastic gradients is assumed to be bounded, i.e.,

$$\|\nabla f_n(w) - \nabla f(w, z_{n,i})\|^2 \leq \sigma_n^2, \forall n \in \mathcal{N}, z_{n,i} \in \mathcal{D}_n, \quad (14)$$

where σ_n^2 represents the local data variance of client n (Huang et al., 2023; Li and Li, 2023). With Equation (14) and $\forall m \in \mathcal{M}, n \in \mathcal{N}_m$, we can further derive

$$\|\nabla f_n(w) - \nabla f(w, \xi_n)\|^2 \leq \sigma_n^2, \forall n \in \mathcal{N}, \quad (15)$$

$$\left\| \sum_{n \in \mathcal{N}_m} \gamma_n^m (\nabla f_n(w) - \nabla f(w, \xi_n)) \right\|^2 \leq \theta_m^2, \forall m \in \mathcal{M} \quad (16)$$

where $\theta_m^2 = \sum_{n \in \mathcal{N}_m} \gamma_n^m \sigma_n^2$. The inequality in Equations (15) and (16) define the variance due to data sampling for one client or one cluster. We also assume

$$\mathbb{E} \|\nabla F(w) - \nabla F_m(w)\|^2 \leq \sigma^2, \forall m \in \mathcal{M}. \quad (17)$$

The inequality in Equation (17) bounds the heterogeneity between global dataset and the dataset in any cluster. In summary, this assumption allows the distribution of dataset in any cluster to be heterogeneous from their peers. When σ^2 goes to zero, the assumed heterogeneity disappears among the clusters. It is also worthy to note that we still assume the existence of data heterogeneity among all the clients, while we just do not impose any constraint on the extent of them, which is more general.

G Proof of Theorem Theorem 4.1

G.1 Key Lemmas

To effectively convey our proofs, we need to prove some useful lemmas in advance. We provide the claim of lemmas in current section, but we defer these lemmas' proof to Appendix I. For convenience, we define $g_k^t = \sum_{n \in \mathcal{N}_{m(t)}} \gamma_n^{m(t)} \nabla f(w_k^t, \xi_{n,k})$, which represents the weighted sum of the local gradients on ES node $m(t)$ after k round of broadcasting in the cluster.

Lemma G.1. Define $\bar{g}_k^t = \mathbb{E}[g_k^t] = \sum_{n \in \mathcal{N}_m(t)} \gamma_n^{m(t)} \nabla f_n(w_k^t)$, then with Assumption F.2, we have

$$\begin{aligned}
-2 \left\langle w^{t-1} - w^*, \sum_{k=0}^{K-1} \eta_k \bar{g}_k^{t-1} \right\rangle &\leq \sum_{k=0}^{K-1} \left(\frac{1}{K} + \mu \eta_k \right) \|w^{t-1} - w_k^{t-1}\|^2 \\
&+ K \sum_{k=0}^{K-1} \eta_k^2 \sum_{n \in \mathcal{N}_m(t-1)} \gamma_n^{m(t-1)} \|\nabla f_n(w_k^{t-1})\|^2 \\
&+ 2 \sum_{k=0}^{K-1} \eta_k \sum_{n \in \mathcal{N}_m(t-1)} \gamma_n^{m(t-1)} (f_n(w^*) - f_n(w_k^{t-1})) \\
&- \frac{\mu}{2} \sum_{k=0}^{K-1} \|w^{t-1} - w^*\|^2 \tag{18}
\end{aligned}$$

Proof. See Appendix I.1 □

Lemma G.2. Suppose $\eta_k < \frac{1}{2LK}$ for $k \in \mathcal{K}$, then we have

$$\begin{aligned}
& - \sum_{k=0}^{K-1} 2\eta_k (1 - 2LK\eta_k) \sum_{n \in \mathcal{N}_m(t-1)} \gamma_n^{m(t-1)} (f_n(w_k^{t-1}) - f_n(w^*)) \\
& \leq \sum_{k=0}^{K-1} 2\eta_k (1 - 2LK\eta_k) (LK\eta_k - 1) \sum_{n \in \mathcal{N}_m(t-1)} \gamma_n^{m(t-1)} (f_n(w^{t-1}) - f_n(w^*)) \\
& + \sum_{k=0}^{K-1} 2LK\eta_k^2 \sum_{n \in \mathcal{N}_m(t-1)} \gamma_n^{m(t-1)} (f_n(w^*) - f_n^*) + \sum_{k=0}^{K-1} \left(\frac{1}{K} - \mu \eta_k \right) \|w_k^{t-1} - w^{t-1}\|^2 \tag{19}
\end{aligned}$$

Proof. See Appendix I.2 □

Lemma G.3. Assume Assumption F.4, we have

$$\|w^{t-1} - w_k^{t-1}\|^2 \leq k \sum_{j=0}^{k-1} \eta_j^2 G^2 + k \sum_{j=0}^{k-1} \eta_j^2 \theta_{m(t-1)}^2 \tag{20}$$

Proof. See Appendix I.3 □

G.2 Completing the Proof of Theorem 4.1

Thanks to the smoothness of global loss function $F(w)$ and the fact that $\nabla F(w^*) = 0$, we have

$$\begin{aligned}
\mathbb{E}\{F(w^t)\} - F(w^*) &\leq \mathbb{E} \langle \nabla F(w^*), w^t - w^* \rangle + \frac{L}{2} \mathbb{E} \|w^t - w^*\|^2 \\
&= \frac{L}{2} \mathbb{E} \|w^t - w^*\|^2 \tag{21}
\end{aligned}$$

Based on the results in Equation (21), for $\|w^t - w^*\|$, there is.

$$\begin{aligned}
\|w^t - w^*\|^2 &= \left\| w^{t-1} - w^* - \sum_{k=0}^{K-1} \eta_k g_k^{t-1} \right\|^2 \\
&= \left\| w^{t-1} - w^* + \sum_{k=0}^{K-1} \eta_k (\bar{g}_k^{t-1} - \bar{g}_k^{t-1} - g_k^{t-1}) \right\|^2 \\
&= \left\| w^{t-1} - w^* - \sum_{k=0}^{K-1} \eta_k \bar{g}_k^{t-1} \right\|^2 + \left\| \sum_{k=0}^{K-1} \eta_k (\bar{g}_k^{t-1} - g_k^{t-1}) \right\|^2 \\
&\quad + 2 \left\langle w^{t-1} - w^* - \sum_{k=0}^{K-1} \eta_k \bar{g}_k^{t-1}, \sum_{k=0}^{K-1} \eta_k (\bar{g}_k^{t-1} - g_k^{t-1}) \right\rangle \tag{22}
\end{aligned}$$

Note that $\mathbb{E}[\bar{g}_k^{t-1} - g_k^{t-1}] = 0$, we have

$$\begin{aligned}
\mathbb{E} \|w^t - w^*\|^2 &= \mathbb{E} \|w^{t-1} - w^*\|^2 + \mathbb{E} \left\| \sum_{k=0}^{K-1} \eta_k (\bar{g}_k^{t-1} - g_k^{t-1}) \right\|^2 \\
&\quad + \mathbb{E} \left\| \sum_{k=0}^{K-1} \eta_k \bar{g}_k^{t-1} \right\|^2 - 2 \mathbb{E} \left\langle w^{t-1} - w^*, \sum_{k=0}^{K-1} \eta_k \bar{g}_k^{t-1} \right\rangle \tag{23}
\end{aligned}$$

By using the Cauchy Schwartz inequality, we have $\sum_{i=1}^n \|a_i b_i\|^2 \leq \sum_{i=1}^n \|a_i\|^2 \sum_{i=1}^n \|b_i\|^2$. And combing the inequality with Equation (23), it follows that

$$\begin{aligned}
\|w^t - w^*\|^2 &\leq \|w^{t-1} - w^*\|^2 - 2 \left\langle w^{t-1} - w^*, \sum_{k=0}^{K-1} \eta_k \bar{g}_k^{t-1} \right\rangle \\
&\quad + K \sum_{k=0}^{K-1} \eta_k^2 \|\bar{g}_k^{t-1}\|^2 + K \sum_{k=0}^{K-1} \eta_k^2 \theta_{m(t-1)}^2 \tag{24}
\end{aligned}$$

where $\theta_{m(t)}^2$ can be checked from Assumption F.4.

From Lemma G.1, it follows that

$$\begin{aligned}
&\|w^t - w^*\|^2 \\
&\leq \left(1 - \frac{\mu}{2} \sum_{k=0}^{K-1} \eta_k \right) \|w^{t-1} - w^*\|^2 + K \sum_{k=0}^{K-1} \eta_k^2 \theta_{m(t-1)}^2 + \sum_{k=0}^{K-1} \left(\frac{1}{K} + \mu \eta_k \right) \|w^{t-1} - w_k^{t-1}\|^2 \\
&\quad + 2K \underbrace{\sum_{k=0}^{K-1} \eta_k^2 \sum_{n \in \mathcal{N}_{m(t-1)}} \gamma_n^{m(t-1)} \|\nabla f_n(w_k^{t-1})\|^2 + 2 \sum_{k=0}^{K-1} \eta_k \sum_{n \in \mathcal{N}_{m(t-1)}} \gamma_n^{m(t-1)} (f_n(w^*) - f_n(w_k^{t-1}))}_{A_1} \tag{25}
\end{aligned}$$

Since $f_n(w)$ is also L-smooth (Li et al., 2020), it follows that

$$\|\nabla f_n(w_k^{t-1})\|^2 \leq 2L (f_n(w_k^{t-1}) - f_n^*) \tag{26}$$

Next, we aim to bound A_1 . By using Equation (26), we have

$$\begin{aligned}
& 2K \sum_{k=0}^{K-1} \eta_k^2 \sum_{n \in \mathcal{N}_m(t-1)} \gamma_n^{m(t-1)} \|\nabla f_n(w_k^{t-1})\|^2 + 2 \sum_{k=0}^{K-1} \eta_k \sum_{n \in \mathcal{N}_m(t-1)} \gamma_n^{m(t-1)} (f_n(w^*) - f_n(w_k^{t-1})) \\
& \leq 4LK \sum_{k=0}^{K-1} \eta_k^2 \sum_{n \in \mathcal{N}_m(t-1)} \gamma_n^{m(t-1)} (f_n(w_k^{t-1}) - f_n^*) \\
& + 2 \sum_{k=0}^{K-1} \eta_k \sum_{n \in \mathcal{N}_m(t-1)} \gamma_n^{m(t-1)} (f_n(w^*) - f_n(w_k^{t-1})) \\
& = \sum_{k=0}^{K-1} 2\eta_k (2LK\eta_k - 1) \sum_{n \in \mathcal{N}_m(t-1)} \gamma_n^{m(t-1)} (f_n(w_k^{t-1}) - f_n^*) \\
& + 2 \sum_{k=0}^{K-1} \eta_k \sum_{n \in \mathcal{N}_m(t-1)} \gamma_n^{m(t-1)} (f_n(w^*) - f_n^*) \\
& = - \sum_{k=0}^{K-1} 2\eta_k (1 - 2LK\eta_k) \sum_{n \in \mathcal{N}_m(t-1)} \gamma_n^{m(t-1)} (f_n(w_k^{t-1}) - f_n^*) \\
& + 2 \sum_{k=0}^{K-1} \eta_k \sum_{n \in \mathcal{N}_m(t-1)} \gamma_n^{m(t-1)} (f_n(w^*) - f_n^*) \\
& = - \underbrace{\sum_{k=0}^{K-1} 2\eta_k (1 - 2LK\eta_k) \sum_{n \in \mathcal{N}_m(t-1)} \gamma_n^{m(t-1)} (f_n(w_k^{t-1}) - f_n(w^*))}_{A_2} \\
& + 4LK \sum_{k=0}^{K-1} \eta_k^2 \sum_{n \in \mathcal{N}_m(t-1)} \gamma_n^{m(t-1)} (f_n(w^*) - f_n^*) \tag{27}
\end{aligned}$$

From Lemma G.2 and Lemma G.3, combining Equation (25) and Equation (27), it follows that

$$\begin{aligned}
\|w^t - w^*\|^2 & \leq \left(1 - \frac{\mu}{2} \sum_{k=0}^{K-1} \eta_k\right) \|w^{t-1} - w^*\|^2 + \sum_{k=0}^{K-1} \left(K\eta_k^2 + \frac{2k}{K} \sum_{j=0}^{k-1} \eta_j^2\right) \theta_{m(t-1)}^2 \\
& + \sum_{k=0}^{K-1} 2\eta_k (1 - 2LK\eta_k) (LK\eta_k - 1) \sum_{n \in \mathcal{N}_m(t-1)} \gamma_n^{m(t-1)} (f_n(w^{t-1}) - f_n(w^*)) \\
& + \sum_{k=0}^{K-1} \frac{2k}{K} \sum_{j=0}^{k-1} \eta_j^2 G^2 + \sum_{k=0}^{K-1} 6LK\eta_k^2 \sum_{n \in \mathcal{N}_m(t-1)} \gamma_n^{m(t-1)} (f_n(w^*) - f_n^*) \tag{28}
\end{aligned}$$

Recalling that

$$\beta = \frac{\mu}{2} \sum_{k=0}^{K-1} \eta_k, \tag{29}$$

$$\Delta_m = \sum_{n \in \mathcal{N}_m} \gamma_n^m (f_n(w^t) - f_n(w^*)), \forall m \in \mathcal{M}, \tag{30}$$

$$\tau_m = \sum_{n \in \mathcal{N}_m} \gamma_n^m (f_n(w^*) - f_n^*), \forall m \in \mathcal{M}, \tag{31}$$

through t rounds of iteration, we have

$$\begin{aligned}
\|w^t - w^*\|^2 &\leq (1 - \beta)^t \|w^0 - w^*\|^2 + \sum_{k=0}^{K-1} \left(K\eta_k^2 + \frac{2k}{K} \sum_{j=0}^{k-1} \eta_j^2 \right) \sum_{i=0}^{t-1} (1 - \beta)^i \theta_{m(i)}^2 \\
&\quad + \sum_{k=0}^{K-1} \frac{2k}{K} \sum_{j=0}^{k-1} \eta_j^2 \sum_{i=0}^{t-1} (1 - \beta)^i G^2 \\
&\quad + \sum_{k=0}^{K-1} 2\eta_k (1 - 2LK\eta_k) (LK\eta_k - 1) \sum_{i=0}^{t-1} (1 - \beta)^i \Delta_{m(i)} \\
&\quad + \sum_{k=0}^{K-1} 6LK\eta_k^2 \sum_{i=0}^{t-1} (1 - \beta)^i \tau_{m(i)}
\end{aligned} \tag{32}$$

And combining the Equation (21) and Equation (32), we bound the $\mathbb{E}\{F(w^T)\} - F(w^*)$

$$\begin{aligned}
\mathbb{E}\{F(w^T)\} - F(w^*) &\leq \frac{L}{2} (1 - \beta)^T \|w^0 - w^*\|^2 + \frac{L}{2} \sum_{k=0}^{K-1} \left(K\eta_k^2 + \frac{2k}{K} \sum_{j=0}^{k-1} \eta_j^2 \right) \sum_{t=0}^{T-1} (1 - \beta)^t \theta_{m(t)}^2 \\
&\quad + \frac{L}{2} \sum_{k=0}^{K-1} 2\eta_k (1 - 2LK\eta_k) (LK\eta_k - 1) \sum_{t=0}^{T-1} (1 - \beta)^t \Delta_{m(t)} \\
&\quad + \frac{L}{2} \sum_{k=0}^{K-1} \frac{2k}{K} \sum_{j=0}^{k-1} \eta_j^2 \sum_{t=0}^{T-1} (1 - \beta)^t G^2 + \frac{L}{2} \sum_{k=0}^{K-1} 6LK\eta_k^2 \sum_{t=0}^{T-1} (1 - \beta)^t \tau_{m(t)}
\end{aligned} \tag{33}$$

This completes the proof.

H Proof of Theorem Theorem 4.3

H.1 Key Lemmas

We first give some necessary lemmas. Their proof are deferred to Appendix I. Firstly, we still denote $g_k^t = \sum_{n \in \mathcal{N}_{m(t)}} \gamma_n^{m(t)} \nabla f(w_k^t, \xi_{n,k})$.

Lemma H.1. *Assume Assumption F.4, it follows that*

$$\mathbb{E} \langle \nabla F(w^t), \nabla F_{m(t)}(w^t) - g_k^t \rangle \leq \frac{1}{4} \mathbb{E} \|\nabla F(w^t)\|^2 + \theta_{m(t)}^2 \tag{34}$$

Proof. See Appendix I.4 □

Lemma H.2. *According to Assumption F.4, it follows that*

$$\mathbb{E} \langle \nabla F(w^t), \nabla F(w^t) - \nabla F_{m(t)}(w^t) \rangle \leq \frac{1}{2} \mathbb{E} \|\nabla F(w^t)\|^2 - \frac{1}{2} \mathbb{E} \|\nabla F_{m(t)}(w^t)\|^2 + \frac{1}{2} \sigma^2 \tag{35}$$

Proof. See Appendix I.5 □

H.2 Completing the Proof of Theorem 4.3

In case the loss function is non-convex, we first have

$$\begin{aligned}
\langle \nabla F(w^t), g_k^t \rangle &= \langle \nabla F(w^t), g_k^t - \nabla F_{m(t)}(w^t) \rangle + \langle \nabla F(w^t), \nabla F_{m(t)}(w^t) - \nabla F(w^t) \rangle \\
&\quad + \langle \nabla F(w^t), \nabla F(w^t) \rangle
\end{aligned} \tag{36}$$

Then there is

$$\begin{aligned} \|\nabla F(w^t)\|^2 &= \langle \nabla F(w^t), g_k^t \rangle + \langle \nabla F(w^t), \nabla F_{m(t)}(w^t) - g_k^t \rangle \\ &\quad + \langle \nabla F(w^t), \nabla F(w^t) - \nabla F_{m(t)}(w^t) \rangle \end{aligned} \quad (37)$$

From Lemma H.1 and Lemma H.2, it follows that

$$\frac{1}{4} \|\nabla F(w^t)\|^2 \leq \langle \nabla F(w^t), g_k^t \rangle + \theta_{m(t)}^2 + \frac{1}{2} \sigma^2 - \frac{1}{2} \|\nabla F_{m(t)}(w^t)\|^2 \quad (38)$$

Therefore, we can get

$$\langle \nabla F(w^t), g_k^t \rangle \geq \frac{1}{4} \|\nabla F(w^t)\|^2 + \frac{1}{2} \|\nabla F_{m(t)}(w^t)\|^2 - \left(\theta_{m(t)}^2 + \frac{1}{2} \sigma^2 \right) \quad (39)$$

Telescoping K rounds of iterations in cluster $m(t)$, it follows that

$$\begin{aligned} \sum_{k=0}^{K-1} \eta_k \langle \nabla F(w^t), g_k^t \rangle &\geq \frac{1}{4} \sum_{k=0}^{K-1} \eta_k \|\nabla F(w^t)\|^2 + \frac{1}{2} \sum_{k=0}^{K-1} \eta_k \|\nabla F_{m(t)}(w^t)\|^2 \\ &\quad - \sum_{k=0}^{K-1} \eta_k \left(\theta_{m(t)}^2 + \frac{1}{2} \sigma^2 \right) \end{aligned} \quad (40)$$

Since $F(w)$ is L -smooth, it follows that

$$\begin{aligned} \sum_{k=0}^{K-1} \eta_k \langle \nabla F(w^t), g_k^t \rangle &= \langle \nabla F(w^t), w^t - w^{t+1} \rangle \\ &\leq F(w^t) - F(w^{t+1}) + \frac{L}{2} \|w^t - w^{t+1}\|^2 \\ &\leq F(w^t) - F(w^{t+1}) + \frac{L}{2} \left\| \sum_{k=0}^{K-1} \eta_k g_k^t \right\|^2 \\ &\leq F(w^t) - F(w^{t+1}) + \frac{LK}{2} \sum_{k=0}^{K-1} \eta_k^2 \|g_k^t\|^2 \\ &\leq F(w^t) - F(w^{t+1}) + \frac{LK}{2} \sum_{k=0}^{K-1} \eta_k^2 \left(\theta_{m(t)}^2 + \|\bar{g}_k^t\|^2 \right) \end{aligned} \quad (41)$$

Combining Equation (40) and Equation (41), it follows that

$$\begin{aligned} \frac{1}{4} \sum_{k=0}^{K-1} \eta_k \|\nabla F(w^t)\|^2 &\leq F(w^t) - F(w^{t+1}) + \left(\frac{LK}{2} \sum_{k=0}^{K-1} \eta_k^2 + \sum_{k=0}^{K-1} \eta_k \right) \theta_{m(t)}^2 \\ &\quad + \sum_{k=0}^{K-1} \left(\frac{LK}{2} \eta_k^2 - \frac{1}{2} \eta_k \right) \|\nabla F_{m(t)}(w^t)\|^2 + \frac{1}{2} \sum_{k=0}^{K-1} \eta_k \sigma^2 \end{aligned} \quad (42)$$

Recalling that $\eta_k \leq \frac{1}{LK}$, divide both sides of the inequality (42) by $\frac{1}{4} \sum_{k=0}^{K-1} \eta_k$, then we have

$$\|\nabla F(w^t)\|^2 \leq \frac{4(F(w^t) - F(w^{t+1}))}{\sum_{k=0}^{K-1} \eta_k} + \left(\frac{2LK \sum_{k=0}^{K-1} \eta_k^2}{\sum_{k=0}^{K-1} \eta_k} + 4 \right) \theta_{m(t)}^2 + 2\sigma^2 \quad (43)$$

Given that the minimum of $\|\nabla F(w^t)\|^2$ for $t = 0, 1, \dots, T-1$ is upper bounded by the average of them, we can bound the minimum of $\|\nabla F(w^t)\|^2$ for $t = 0, 1, \dots, T-1$ as follows

$$\begin{aligned}
& \mathbb{E} \left[\frac{1}{T} \sum_{t=0}^{T-1} \|\nabla F(w^t)\|^2 \right] \\
& \leq \frac{1}{T} \sum_{t=0}^{T-1} \frac{4(F(w^t) - F(w^{t+1}))}{\sum_{k=0}^{K-1} \eta_k} + \left(\frac{2LK \sum_{k=0}^{K-1} \eta_k^2}{\sum_{k=0}^{K-1} \eta_k} + 4 \right) \frac{1}{T} \sum_{t=0}^{T-1} \theta_{m(t)}^2 + \frac{2}{T} \sum_{t=0}^{T-1} \sigma^2 \\
& \leq \frac{4[F(w^0) - F(w^*)]}{T \sum_{k=0}^{K-1} \eta_k} + \left(\frac{2LK \sum_{k=0}^{K-1} \eta_k^2}{\sum_{k=0}^{K-1} \eta_k} + 4 \right) \frac{1}{T} \sum_{t=0}^{T-1} \theta_{m(t)}^2 + \frac{2}{T} \sum_{t=0}^{T-1} \sigma^2 \tag{44}
\end{aligned}$$

Since $F(w^*)$ be the global minimum of the loss function $F(w)$, then there is

$$F(w^0) - F(w^t) \leq F(w^0) - F(w^*) \tag{45}$$

Combining Equation (44) and Equation (45), we have

$$\mathbb{E} \left[\frac{1}{T} \sum_{t=0}^{T-1} \|\nabla F(w^t)\|^2 \right] \leq \frac{4[F(w^0) - F(w^*)]}{T \sum_{k=0}^{K-1} \eta_k} + \left(\frac{2LK \sum_{k=0}^{K-1} \eta_k^2}{\sum_{k=0}^{K-1} \eta_k} + 4 \right) \frac{1}{T} \sum_{t=0}^{T-1} \theta_{m(t)}^2 + \frac{2}{T} \sum_{t=0}^{T-1} \sigma^2 \tag{46}$$

This completes the proof.

I Deferred Proof of Lemmas

I.1 Proof of Lemma G.1

Splitting and expanding the left-hand side of Equation (18), we can get

$$\begin{aligned}
-2 \left\langle w^{t-1} - w^*, \sum_{k=0}^{K-1} \eta_k \bar{g}_k^{t-1} \right\rangle &= -2 \sum_{k=0}^{K-1} \eta_k \left\langle w^{t-1} - w^*, \sum_{n \in \mathcal{N}_m(t-1)} \gamma_n^{m(t-1)} \nabla f_n(w_k^{t-1}) \right\rangle \\
&= -2 \underbrace{\sum_{k=0}^{K-1} \eta_k \left\langle w^{t-1} - w_k^{t-1}, \sum_{n \in \mathcal{N}_m(t-1)} \gamma_n^{m(t-1)} \nabla f_n(w_k^{t-1}) \right\rangle}_{C_1} \\
&= -2 \underbrace{\sum_{k=0}^{K-1} \eta_k \left\langle w_k^{t-1} - w^*, \sum_{n \in \mathcal{N}_m(t-1)} \gamma_n^{m(t-1)} \nabla f_n(w_k^{t-1}) \right\rangle}_{C_2} \tag{47}
\end{aligned}$$

By using Cauchy Schwartz and AM-GM inequality (Nguyen et al., 2022), we can bound C_1

$$\begin{aligned}
& -2 \sum_{k=0}^{K-1} \eta_k \left\langle w^{t-1} - w_k^{t-1}, \sum_{n \in \mathcal{N}_m(t-1)} \gamma_n^{m(t-1)} \nabla f_n(w_k^{t-1}) \right\rangle \\
& \leq \sum_{k=0}^{K-1} \eta_k \left[\frac{1}{K\eta_k} \|w^{t-1} - w_k^{t-1}\|^2 + K\eta_k \left\| \sum_{n \in \mathcal{N}_m(t-1)} \gamma_n^{m(t-1)} \nabla f_n(w_k^{t-1}) \right\|^2 \right] \\
& = \frac{1}{K} \sum_{k=0}^{K-1} \|w^{t-1} - w_k^{t-1}\|^2 + K \sum_{k=0}^{K-1} \eta_k^2 \sum_{n \in \mathcal{N}_m(t-1)} \gamma_n^{m(t-1)} \|\nabla f_n(w_k^{t-1})\|^2 \tag{48}
\end{aligned}$$

Because of the strong convexity of $f_n(w)$ for $n \in \mathcal{N}_m(t-1)$, we have

$$\begin{aligned}
& -2 \sum_{k=0}^{K-1} \eta_k \left\langle w_k^{t-1} - w^*, \sum_{n \in \mathcal{N}_m(t-1)} \gamma_n^{m(t-1)} \nabla f_n(w_k^{t-1}) \right\rangle \\
& \leq 2 \sum_{k=0}^{K-1} \eta_k \sum_{n \in \mathcal{N}_m(t-1)} \gamma_n^{m(t-1)} (f_n(w^*) - f_n(w_k^{t-1})) - \mu \sum_{k=0}^{K-1} \eta_k \|w_k^{t-1} - w^*\|^2 \quad (49)
\end{aligned}$$

By using Cauchy Schwartz inequality, we have

$$-\mu \sum_{k=0}^{K-1} \eta_k \|w_k^{t-1} - w^*\|^2 \leq \mu \sum_{k=0}^{K-1} \eta_k \left[\|w_k^{t-1} - w^{t-1}\|^2 - \frac{1}{2} \|w^{t-1} - w^*\|^2 \right] \quad (50)$$

We combine Equation (47), Equation (48), Equation (49) and Equation (50), it follows that

$$\begin{aligned}
& -2 \left\langle w^{t-1} - w^*, \sum_{k=0}^{K-1} \eta_k \bar{g}_k^{t-1} \right\rangle \\
& \leq \sum_{k=0}^{K-1} \left(\frac{1}{K} + \mu \eta_k \right) \|w^{t-1} - w_k^{t-1}\|^2 + K \sum_{k=0}^{K-1} \eta_k^2 \sum_{n \in \mathcal{N}_m(t-1)} \gamma_n^{m(t-1)} \|\nabla f_n(w_k^{t-1})\|^2 \\
& + 2 \sum_{k=0}^{K-1} \eta_k \sum_{n \in \mathcal{N}_m(t-1)} \gamma_n^{m(t-1)} (f_n(w^*) - f_n(w_k^{t-1})) - \frac{\mu}{2} \sum_{k=0}^{K-1} \|w^{t-1} - w^*\|^2 \quad (51)
\end{aligned}$$

This completes the proof.

I.2 Proof of Lemma G.2

We can split Equation (19) into two terms, it follows that

$$\begin{aligned}
& - \sum_{k=0}^{K-1} 2\eta_k (1 - 2LK\eta_k) \sum_{n \in \mathcal{N}_m(t-1)} \gamma_n^{m(t-1)} (f_n(w_k^{t-1}) - f_n(w^*)) \\
& = - \underbrace{\sum_{k=0}^{K-1} 2\eta_k (1 - 2LK\eta_k) \sum_{n \in \mathcal{N}_m(t-1)} \gamma_n^{m(t-1)} (f_n(w_k^{t-1}) - f_n(w^{t-1}))}_{C_3} \\
& - \sum_{k=0}^{K-1} 2\eta_k (1 - 2LK\eta_k) \sum_{n \in \mathcal{N}_m(t-1)} \gamma_n^{m(t-1)} (f_n(w^{t-1}) - f_n(w^*)) \quad (52)
\end{aligned}$$

Attributed to the strong convexity of $f_n(w)$, we have

$$f_n(w_k^{t-1}) - f_n(w^{t-1}) \geq \langle \nabla f_n(w^{t-1}), w_k^{t-1} - w^{t-1} \rangle + \frac{\mu}{2} \|w_k^{t-1} - w^{t-1}\|^2 \quad (53)$$

Combing Equation (53) with C_3 , we have

$$\begin{aligned}
& - \sum_{k=0}^{K-1} 2\eta_k (1 - 2LK\eta_k) \sum_{n \in \mathcal{N}_m(t-1)} \gamma_n^{m(t-1)} (f_n(w_k^{t-1}) - f_n(w^{t-1})) \\
& \leq -\mu \sum_{k=0}^{K-1} \eta_k (1 - 2LK\eta_k) \sum_{n \in \mathcal{N}_m(t-1)} \gamma_n^{m(t-1)} \|w_k^{t-1} - w^{t-1}\|^2 \\
& - \sum_{k=0}^{K-1} 2\eta_k (1 - 2LK\eta_k) \sum_{n \in \mathcal{N}_m(t-1)} \gamma_n^{m(t-1)} \langle \nabla f_n(w^{t-1}), w_k^{t-1} - w^{t-1} \rangle \quad (54)
\end{aligned}$$

By using Cauchy Schwartz inequality, we have

$$\begin{aligned}
& - \sum_{k=0}^{K-1} 2\eta_k (1 - 2LK\eta_k) \sum_{n \in \mathcal{N}_m(t-1)} \gamma_n^{m(t-1)} \langle \nabla f_n(w^{t-1}), w_k^{t-1} - w^{t-1} \rangle \\
& \leq \sum_{k=0}^{K-1} 2\eta_k (1 - 2LK\eta_k) \sum_{n \in \mathcal{N}_m(t-1)} \gamma_n^{m(t-1)} \left(\frac{K\eta_k}{2} \|f_n(w^{t-1})\|^2 + \frac{1}{2K\eta_k} \|w_k^{t-1} - w^{t-1}\|^2 \right)
\end{aligned} \tag{55}$$

Combining Equation (54) and Equation (55), we can bound C_3

$$\begin{aligned}
& - \sum_{k=0}^{K-1} 2\eta_k (1 - 2LK\eta_k) \sum_{n \in \mathcal{N}_m(t-1)} \gamma_n^{m(t-1)} (f_n(w_k^{t-1}) - f_n(w^{t-1})) \\
& \leq \sum_{k=0}^{K-1} 2LK\eta_k^2 (1 - 2LK\eta_k) \sum_{n \in \mathcal{N}_m(t-1)} \gamma_n^{m(t-1)} (f_n(w^{t-1}) - f_n^*) \\
& \quad + \sum_{k=0}^{K-1} \left(\frac{1}{K} - \mu\eta_k \right) (1 - 2LK\eta_k) \sum_{n \in \mathcal{N}_m(t-1)} \gamma_n^{m(t-1)} \|w_k^{t-1} - w^{t-1}\|^2
\end{aligned} \tag{56}$$

Next, by combining Equation (52) and Equation (56), it follows that

$$\begin{aligned}
& - \sum_{k=0}^{K-1} 2\eta_k (1 - 2LK\eta_k) \sum_{n \in \mathcal{N}_m(t-1)} \gamma_n^{m(t-1)} (f_n(w_k^{t-1}) - f_n(w^*)) \\
& \leq \sum_{k=0}^{K-1} 2LK\eta_k^2 (1 - 2LK\eta_k) \sum_{n \in \mathcal{N}_m(t-1)} \gamma_n^{m(t-1)} (f_n(w^{t-1}) - f_n^*) \\
& \quad - \underbrace{\sum_{k=0}^{K-1} 2\eta_k (1 - 2LK\eta_k) \sum_{n \in \mathcal{N}_m(t-1)} \gamma_n^{m(t-1)} (f_n(w^{t-1}) - f_n(w^*))}_{C_4} \\
& \quad + \sum_{k=0}^{K-1} \left(\frac{1}{K} - \mu\eta_k \right) (1 - 2LK\eta_k) \sum_{n \in \mathcal{N}_m(t-1)} \gamma_n^{m(t-1)} \|w_k^{t-1} - w^{t-1}\|^2
\end{aligned} \tag{57}$$

Note that

$$\begin{aligned}
C_4 & \leq \sum_{k=0}^{K-1} 2\eta_k (1 - 2LK\eta_k) (LK\eta_k - 1) \sum_{n \in \mathcal{N}_m(t-1)} \gamma_n^{m(t-1)} (f_n(w^{t-1}) - f_n(w^*)) \\
& \quad + \sum_{k=0}^{K-1} 2LK\eta_k^2 (1 - 2LK\eta_k) \sum_{n \in \mathcal{N}_m(t-1)} \gamma_n^{m(t-1)} (f_n(w^*) - f_n^*)
\end{aligned} \tag{58}$$

Combining Equation (57) and Equation (58), we have

$$\begin{aligned}
& - \sum_{k=0}^{K-1} 2\eta_k (1 - 2LK\eta_k) \sum_{n \in \mathcal{N}_m(t-1)} \gamma_n^{m(t-1)} (f_n(w_k^{t-1}) - f_n(w^*)) \\
& \leq \sum_{k=0}^{K-1} 2\eta_k (1 - 2LK\eta_k) (LK\eta_k - 1) \sum_{n \in \mathcal{N}_m(t-1)} \gamma_n^{m(t-1)} (f_n(w^{t-1}) - f_n(w^*)) \\
& + \sum_{k=0}^{K-1} 2LK\eta_k^2 (1 - 2LK\eta_k) \sum_{n \in \mathcal{N}_m(t-1)} \gamma_n^{m(t-1)} (f_n(w^*) - f_n^*) \\
& + \sum_{k=0}^{K-1} \left(\frac{1}{K} - \mu\eta_k \right) (1 - 2LK\eta_k) \sum_{n \in \mathcal{N}_m(t-1)} \gamma_n^{m(t-1)} \|w_k^{t-1} - w^{t-1}\|^2 \tag{59}
\end{aligned}$$

Given that $\eta_k < \frac{1}{2LK}$ for $k \in \mathcal{K}$, it follows that

$$\begin{aligned}
& - \sum_{k=0}^{K-1} 2\eta_k (1 - 2LK\eta_k) \sum_{n \in \mathcal{N}_m(t-1)} \gamma_n^{m(t-1)} (f_n(w_k^{t-1}) - f_n(w^*)) \\
& \leq \sum_{k=0}^{K-1} 2\eta_k (1 - 2LK\eta_k) (LK\eta_k - 1) \sum_{n \in \mathcal{N}_m(t-1)} \gamma_n^{m(t-1)} (f_n(w^{t-1}) - f_n(w^*)) \\
& + \sum_{k=0}^{K-1} 2LK\eta_k^2 \sum_{n \in \mathcal{N}_m(t-1)} \gamma_n^{m(t-1)} (f_n(w^*) - f_n^*) \\
& + \sum_{k=0}^{K-1} \left(\frac{1}{K} - \mu\eta_k \right) \|w_k^{t-1} - w^{t-1}\|^2 \tag{60}
\end{aligned}$$

This completes the proof.

I.3 Proof of Lemma G.3

Notice that $w_k^{t-1} = w^{t-1} - \sum_{j=0}^{k-1} \eta_j g_j^{t-1}$, then

$$\begin{aligned}
\|w^{t-1} - w_k^{t-1}\|^2 & \leq \left\| \sum_{j=0}^{k-1} \eta_j g_j^{t-1} \right\|^2 \\
& \leq k \sum_{j=0}^{k-1} \eta_j^2 \|g_j^{t-1}\|^2 \\
& \leq k \sum_{j=0}^{k-1} \eta_j^2 \|g_j^{t-1} - \bar{g}_j^{t-1} + \bar{g}_j^{t-1}\|^2 \\
& \leq k \sum_{j=0}^{k-1} \eta_j^2 \|\bar{g}_j^{t-1}\|^2 + 2k \sum_{j=0}^{k-1} \langle \bar{g}_j^{t-1}, g_j^{t-1} - \bar{g}_j^{t-1} \rangle + k \sum_{j=0}^{k-1} \eta_j^2 \|g_j^{t-1} - \bar{g}_j^{t-1}\|^2 \\
& \leq k \sum_{j=0}^{k-1} \eta_j^2 \|\bar{g}_j^{t-1}\|^2 + k \sum_{j=0}^{k-1} \eta_j^2 \|g_j^{t-1} - \bar{g}_j^{t-1}\|^2 \tag{61}
\end{aligned}$$

Based on the Assumption F.3 and Assumption F.4, we have

$$\|w^{t-1} - w_k^{t-1}\|^2 \leq k \sum_{j=0}^{k-1} \eta_j^2 G^2 + k \sum_{j=0}^{k-1} \eta_j^2 \theta_{m(t-1)}^2 \tag{62}$$

This completes the proof.

I.4 Proof of Lemma H.1

By using Cauchy-Schwartz inequality and AM-GM inequality (Nguyen et al., 2022), it follows that

$$\langle \nabla F(w^t), \nabla F_{m(t)}(w^t) - g_k^t \rangle \leq \frac{1}{4} \mathbb{E} \|\nabla F(w^t)\|^2 + \|\nabla F_{m(t)}(w^t) - g_k^t\|^2 \quad (63)$$

From Assumption F.4, we have

$$\mathbb{E} \|\nabla F_{m(t)}(w^t) - g_k^t\|^2 \leq \mathbb{E} \left\| \sum_{n \in \mathcal{N}_{m(t)}} \gamma_n^{m(t)} (\nabla f_n(w) - \nabla f(w, \xi_{n,k})) \right\|^2 \leq \theta_{m(t)}^2 \quad (64)$$

Combining Equation (63) and Equation (64), it follows that

$$\mathbb{E} \langle \nabla F(w^t), \nabla F_{m(t)}(w^t) - g_k^t \rangle \leq \frac{1}{4} \mathbb{E} \|\nabla F(w^t)\|^2 + \theta_{m(t)}^2 \quad (65)$$

This completes the proof.

I.5 Proof of Lemma H.2

For any two vectors a and b , we have $2a^T b = \|a\|^2 + \|b\|^2 - \|a - b\|^2$. Therefore we can split $\langle \nabla F(w^t), \nabla F(w^t) - \nabla F_{m(t)}(w^t) \rangle$ into three terms

$$\begin{aligned} \mathbb{E} \langle \nabla F(w^t), \nabla F(w^t) - \nabla F_{m(t)}(w^t) \rangle &= \frac{1}{2} \mathbb{E} \|\nabla F(w^t)\|^2 - \frac{1}{2} \mathbb{E} \|\nabla F_{m(t)}(w^t)\|^2 \\ &\quad + \frac{1}{2} \mathbb{E} \|\nabla F(w^t) - \nabla F_{m(t)}(w^t)\|^2 \end{aligned} \quad (66)$$

According to Assumption F.4, it follows that

$$\mathbb{E} \langle \nabla F(w^t), \nabla F(w^t) - \nabla F_{m(t)}(w^t) \rangle \leq \frac{1}{2} \mathbb{E} \|\nabla F(w^t)\|^2 - \frac{1}{2} \mathbb{E} \|\nabla F_{m(t)}(w^t)\|^2 + \frac{1}{2} \sigma^2 \quad (67)$$

This completes the proof.